UNIVERSITÉ DE MONTRÉAL

WIDEBAND TRANSFER FUNCTION IDENTIFICATION USING MAGVF (MAGNITUDE VECTOR FITTING) METHOD

NAVEEN GOSWAMY
DÉPARTEMENT DE GÉNIE ÉLECTRIQUE
ÉCOLE POLYTECHNIQUE DE MONTRÉAL

MÉMOIRE PRÉSENTÉ EN VUE DE L'OBTENTION
DU DIPLÔME DE MAÎTRISE ÈS SCIENCES APPLIQUÉES
(GÉNIE ÉLECTRIQUE)
AOÛT 2013

UNIVERSITÉ DE MONTRÉAL

ÉCOLE POLYTECHNIQUE DE MONTRÉAL

Ce mémoire intitulé:

WIDEBAND TRANSFER FUNCTION IDENTIFICATION USING MAGVF (MAGNITUDE VECTOR FITTING) METHOD

présenté par: GOSWAMY Naveen
en vue de l'obtention du diplôme de: Maîtrise ès sciences appliquées
a été dûment accepté par le jury d'examen constitué de:

M. MAHSEREDJIAN Jean, Ph.D., président
M. KOCAR Ilhan, Ph.D., membre et directeur de recherche
M. KARIMI Houshang, Ph.D., membre

I dedicate this to my family,
in recognition of the sacrifices
that permitted me to reach further.

ACKNOWLEDGEMENTS

Many thanks to my academic supervisor, Professor Ilhan Kocar, for his wisdom, support, and friendship.

Thanks as well to the jury members, Professors Jean Mahseredjian and Houshang Karimi, for their guidance and insight.

I am also very grateful to BBA for providing the Bourse Fonds Maurice Brisson, which made it possible for me to realize my studies more easily.

Furthermore, I would like to thank my supervisors and co-workers at the CanmetENERGY research center in Varennes, for providing a welcoming and stimulating work environment, full of opportunities and interesting challenges.

But most of all, I would like to thank my family and friends for their continuous support and love – especially my dearest Marie-Neige, the most wonderful Sanika, and my parents, Rita and Suresh, to whom I am eternally grateful.

RÉSUMÉ

La technique de lissage vectoriel («Vector Fitting»), lorsqu'elle est utilisée avec le modèle universel de ligne (ULM, «Universal Line Model»), sert à identifier les fonctions associées avec les lignes de transport et câbles, soit la fonction matricielle de propagation et l'admittance caractéristique, sous forme de fonctions de transfert dans le domaine fréquentiel. L'un des défis avec cette technique est relié aux calculs complexes requis pour estimer les délais de la fonction de propagation avant d'identifier ses pôles.

Cette mémoire examine la technique de lissage vectoriel de magnitude («Magnitude Vector Fitting» ou «magVF») par rapport à la technique de lissage vectoriel dans l'identification des fonctions modales de propagation. Les valeurs propres de la fonction matricielle de propagation correspondent aux fonctions modales de propagation et chacune des fonctions modales est associée avec un délai. Le modèle ULM propose que chacune des fonctions modales de propagation découplées est un système de phase minimum multiplié par un délai constant dans le domaine fréquentiel. La méthode de lissage vectoriel est utilisée pour obtenir la fonction de transfert des fonctions modales en solutionnant deux équations linéaires séquentielles de moindres carrés. Néanmoins, une approche itérative bouclée doit être utilisée afin de trouver un délai adéquat, tout en minimisant l'erreur d'approximation.

Alternativement, la technique de lissage vectoriel de magnitude est basé sur la technique de lissage vectoriel mais utilise des fonctions de base symétriques pour effectuer le lissage sur une réponse particulière: carrée de la magnitude. Naturellement, l'effet du délai disparait lors de la construction de la réponse à partir de la carrée de magnitude comme entrée pour le lissage. L'utilisation de la technique de lissage vectoriel de magnitude ne nécessite donc pas l'estimation des délais. Le délai d'une fonction modale peut se trouver suite au lissage en faisant des comparaisons de phase entre la fonction obtenue et la fonction originale. Une fois toutes les fonctions modales de propagation sont identifiées avec une tolérance d'erreur prédéfinie, le modèle ULM permet l'utilisation des pôles et délais pour résoudre un dernier problème de moindres carrés afin d'obtenir les résidus de la matrice de propagation dans le domaine de phase.

Afin d'améliorer la qualité et la stabilité d'approximation, une approche de pondération est présentée dans cette étude pour dériver une méthode de lissage vectoriel pondéré de magnitude. Cette étude compare l'algorithme de lissage vectoriel de magnitude avec celui de lissage vectoriel, avec et sans pondération, en faisant des comparaisons en utilisant des vrais données de lignes de transmission. Cette recherche démontre que même si l'algorithme de lissage vectoriel de magnitude élimine le besoin d'estimer les délais avant le lissage, il exige

quand même un calcul supplémentaire pour tenir compte des problèmes numériques. Une étape de modification de pôles à l'entrée est proposée dans ce travail afin de soulager les problèmes numériques.

Il est observé qu'il est possible d'identifier les fonctions modales de propagation par des fonctions de phase minimum avec la méthode de lissage vectoriel de magnitude; par contre, le lissage vectoriel ne garantit pas des systèmes de phase minimum. Il est aussi démontré que les problèmes numériques sont plus manifestants dans le cas des câbles où la dépendance fréquentielle des paramètres est plus importante et complexe.

ABSTRACT

Vector Fitting (VF), when employed with the Universal Line Model (ULM), can be used for approximating system equations of multi-conductor power transmission lines and cables, by helping to identify the propagation matrices and characteristic admittances. However, one of the challenges posed by this technique is the additional computational logic required to estimate the time-delays associated with the modal propagation transfer functions in the frequency domain, prior to arriving at a suitable estimation for poles and residues.

This thesis examines Magnitude Vector Fitting (magVF) as an alternative to VF for the fitting of propagation modes. The ULM employs frequency domain decomposition of n-conductor transmission lines or cables into n-propagation modal propagation functions, each of which has an associated delay. This model proposes that the decoupled modal propagation functions are time-delayed minimum-phase systems in the frequency domain. The VF method is used to fit the individual modal equations in residues-poles form using two sequential linear least-squares problems, but an iterative approach must be employed in order to first establish a suitable time delay while minimizing error in the fitter.

Alternatively, magVF is an algorithm based on VF that uses symmetric basis functions to perform least-squares fitting based on a given squared-magnitude response. Any effect from the delays on the phase is cancelled during the construction of the magnitude-squared response used as input for the fitter. Naturally, the effect of the delays disappears during the construction of the magnitude-squared response. Using magVF does not, therefore, require estimation of time-delays before getting a successful magnitude-squared fit. The time delay of a modal propagation function can then be directly identified by comparing the phase of the resulting fit with that of the desired response. Once all modal propagation functions have been fit within a suitable margin of error, then the ULM model allows the discovered poles and time-delays to be used to solve a final least-squares problem to get the residues of the phase-domain propagation matrix.

A weighting technique that improves the iterative stability and numerical precision of the magVF algorithm known as Weighted Magnitude Vector Fitting (WmagVF) is presented in this study. This study compares the magVF algorithm with the VF one, with and without weighting, and tested against practical transmission line data. This research demonstrates that although the magVF algorithm eliminates the need for doing time-delay estimation prior to fitting, it does require additional logic for dealing with some problems that can arise numerically, making it difficult to implement for certain cases. An Input Pole Modification (IPM) step is proposed and demonstrated. Details are provided for the algorithms of these

methods, and results are presented relative to practical transmission line frequency spectrum data.

It is observed that while magVF restricts the resulting propagation mode equation to be minimum-phase, VF does not guarantee minimum-phase systems. It is also shown that numerical problems are more apparent in cable cases, where the frequency dependence of the fitting parameters becomes more important and complex.

TABLE OF CONTENTS

LIST OF TABLES

LIST OF FIGURES

LIST OF ALGORITHMS

NOMENCLATURE

MAE_1	Maximum Absolute Error of magnitude response (does not include phase response)
MAE_2	Maximum Absolute Error of frequency response (magnitude and phase components are included)
$RMSE_1$	Root Mean Squared Error of magnitude response (does not include phase response)
$RMSE_2$	Root Mean Squared Error of frequency response (magnitude and phase components are included)
EMT	Electro-Magnetic Transients
FS	Final Sweep
i	current iteration
IPM	Input Pole Modification
j	complex operator
LHP	Left Hand s-Plane
LTI	Linear Time-Invariant
magVF	Magnitude Vector Fitting
MPF	Modal Propagation Function
MPS	Minimum Phase System
Norder	Number of poles used when fitting
PFE	Partial Fraction Expansion
RHP	Right Hand s-Plane
SERA	Series of input poles
SERC	Series of residues

SERD	Series of direct terms
SERE	Series of proportional terms
VF	Vector Fitting
W/magVF	Magnitude Vector Fitting, with and/or without Weighting
W/VF	Vector Fitting, with and/or without Weighting
WmagVF	Weighted Magnitude Vector Fitting
WVF	Weighted Vector Fitting

CHAPTER 1

INTRODUCTION

1.1 Overview

This thesis provides an examination of the Magnitude Vector Fitting (magVF) method for the approximation of transfer functions, with particular attention toward the modal propagation functions for power transmission lines and cables. The magVF method is a formulation derived from the original Vector Fitting (VF) method. Since its inception, VF has proven to be a reliable method for macromodeling LTI transfer functions based on system frequency responses. It has been employed in various contexts, and has been integrated in EMT-type programs for the modelling of cable and transmission line propagation functions. The magVF method uses much of the same internal structure as the VF method, but it has been re-designed to use symmetric basis functions which improve the performance when fitting magnitude-squared complex responses.

This thesis presents a study of the magVF method, with some new techniques based on Weighted Vector Fitting (WVF). It also introduces a new Input Pole Modification (IPM) step, that can help to encourage certain types of solutions. Overall, this thesis attempts to better understand the mechanics of these methods, their strengths and limitations, and open up avenues for future research.

1.2 Motivation

One of the limitations of the current VF-based methods when used to approximate propagation functions is the iterative approach required to resolve the time delays that are inherent in the modal decompositions. The magVF method offers an interesting alternative by virtue of its ability to fit the modal propagation functions without needing to first approximate the delays. The magVF algorithm can be used to derive transfer functions when only magnitude response data is known. Furthermore, magVF ensures minimum-phase approximations, which are considered to be a basic building block of cable and transmission line propagation transfer functions.

1.3 Contributions of this thesis

This study investigates the application of magVF for approximating propagation functions, as a replacement for VF methods which are currently employed by EMT-type solutions. Limitations of the algorithm are considered. Modifications are made to produce WmagVF, a new method, based on the synthesis of WVF and magVF. A new Input Pole Modification (IPM) technique is proposed and demonstrated. Performance is compared between the various fitters and modifications. Test results and discussion are provided based on approximations of actual transmission line and cable data.

1.4 Methodology

This thesis implements the magVF technique and tests it with actual cable and transmission line modal data. Modifications are introduced to magVF to provide greater accuracy and allow for improved results via a weighting method. A new pole modification scheme is also introduced to improve iterative success.

The methodology employed was as follows.

1. Study of the state of the art, namely VF, WVF, and magVF methodologies presented in the academic record.
2. Determine algorithm for WmagVF, and implement in MATLAB.
3. Tests of algorithms against various defined transfer functions to discover limitations.
4. Tests of algorithms against practical transmission line and cable propagation functions.
5. Analysis of results
6. Conclusions

CHAPTER 2

STATE OF THE ART

2.1 Literature Review

The term Vector Fitting was initially used in the context of transfer function identification in 1999 by Gustavsen and Semylen [1]. Their research was influenced by an earlier work [2], where a procedure known as Sanathanan-Koerner (S-K) iterations demonstrated how to synthesize a transfer function as a ratio of two complex polynomials based on polynomial curve fitting. S-K iterations method built upon Levy's paper [3] published in 1959 which showed how complex curve fitting problems could be solved effectively using linear systems and matrix formulations, with the foresight to conclude that this approach would be effective in the oncoming age of computational methods.

The VF procedure provides a compact and effective algorithm for automated identification of transfer functions in the classical residues-poles form: as a series of first-order rational expressions in the Laplace domain using two sequential overdetermined linear least-squares problems solved iteratively using a partial fraction basis. The approach was treated in further detail in [4, 5, 6, 7, 8] and many other academic articles since.

Researchers have been inspired to employ and improve the VF technique. In [9, 10] the authors were able to demonstrate that by including an inherent weighting factor that updated after each iteration, it was possible to improve the performance of the fitter. They called this method Weighted Vector Fitting (WVF), and in their analysis presented a modified derivation from that of the original VF algorithm, with results of transfer function determination using the wideband model for underground power cables and transmission lines.

Alternate branches of VF have emerged, in attempts to further develop the utility of the methodology and improve its application. The magVF procedure was published by De Tomassi, Gustavsen, and Dhaene in 2010 [11] and based on a series of works including [12, 13, 14, 15]. In addition to being heavily based on VF, theoretical foundation can be attributed to the 1977 work of Jong and Shanmugam [16], and there is also the 2002 work of Zhang [17] where VF was directly applied to magnitude squared data.

An advantage of magVF is that for minimum-phase systems only the magnitude data is required to arrive at a good approximation, due to the predictable phase of this class of systems. Furthermore, as all systems can be characterized by their magnitude response and phase response, they can also be decomposed into a minimum-phase transfer function

cascaded with an all-pass component. Hence this technique can be ported to many systems where phase data is known or can be otherwise computed.

The transmission line and cable data theory employed in this study is derived from the Frequency Domain [18] based Universal Line Model [19, 20]. This model decomposes the Multiple-Input-Multiple-Output (MIMO) Laplace domain form of the transmission line propagation function down into modal components which can be individually approximated as decoupled minimum-phase Single-Input-Single-Output (SISO) transfer functions with their own respective time delays.

2.2 Modal decomposition of transmission lines and cables

Using distributed parameters, transmission line and cable voltage-current characteristics are described by the Universal Line Model (ULM) using two phase domain matrix transfer functions, namely the propagation matrix $\mathbf{H}$ and characteristic admittance matrix $\mathbf{Y_c}$, which are given as

$$\mathbf{H} = e^{-\sqrt{\mathbf{YZ}}l}, \text{ and} \tag{2.1}$$

$$\mathbf{Y_c} = \mathbf{Z}^{-1}\sqrt{\mathbf{ZY}}, \tag{2.2}$$

where l indicates the length of the line [18, 19]. The matrices $\mathbf{Y}$ and $\mathbf{Z}$ are, respectively, the shunt admittances and series impedances per unit length. These matrices are of size $N_c \times N_c$ where N_c is the number of conductors in the line.

The propagation and characteristic admittance transfer functions allow the calculation of the voltage ($\mathbf{V}$) and current ($\mathbf{I}$) with two ends s and r of a transmission line as shown below

$$\mathbf{I}_r = \mathbf{Y_c}\mathbf{V}_r - \mathbf{H}(\mathbf{Y_c}\mathbf{V}_s + \mathbf{I}_s) \tag{2.3}$$

$$\mathbf{I}_s = \mathbf{Y_c}\mathbf{V}_s - \mathbf{H}(\mathbf{Y_c}\mathbf{V}_r + \mathbf{I}_r) \tag{2.4}$$

These equations are in the steady-state frequency domain, and time-domain results can also be obtained via inverse Fourier transformations.

Furthermore, via modal decomposition, it is possible to represent the MIMO propagation transfer function $\mathbf{H}$ through its modal propagation functions H_m where $m = 1, 2, ..., N_c$. The problem then gets simplified to fitting each of the modes as a decoupled SISO system transfer function with a delay, in the form

$$H_m = H'_m e^{-s\tau_m} \tag{2.5}$$

where τ_m signifies the associated time delay for the modal domain equation H'_m corresponding with mode m, which is proposed to be a minimum phase system [19].

By the residue-pole form that is output from the VF method, H'_m is

$$H'_m = \sum_{n=1}^{N_m} \frac{c_n}{s - p_n} \tag{2.6}$$

where N_m is the order of the approximation (number of poles) used for modal propagation function m.

In [19] it is proposed that the poles of H_m – and hence its minimum phase component H'_m – are the same as the poles used to reconstruct $\mathbf{H}$ as a MIMO system matrix. Supposing that there are N_m poles for the modal propagation function m, and that there are N_c modes in total, then, getting back to the frequency domain from the modal domain involves recomposing the MIMO propagation function as follows.

$$\mathbf{H} \cong \sum_{m=1}^{N_c} \left(\sum_{n=1}^{N_m} \frac{\mathbf{C_{nm}}}{s - p_{nm}} \right) e^{-s\tau_m} \tag{2.7}$$

Once a poles-residues series form of the minimum-phase H'_m with the associated time delay τ_m has been established, then finding the residues $\mathbf{C_{nm}}$ can be done using overdetermined linear systems equations with partial fraction basis functions for another set of linear least squares problems.

2.3 Transfer function identification from tabulated frequency response

For the uninitiated reader, it may be useful to provide some context as to how the fitting algorithms described in this study are generally used. Essentially, the goal is to provide a Laplace domain LTI transfer function represented by the approximation $\widetilde{F}(s_k)$ that can closely approximate the tabulated frequency response of a given system vector $F(s_k)$ over a frequency sequence $s_k = j\omega_k$ where $k = 1, 2, ..., K$.

Representing this system function in terms of a partial fraction series with direct (d) and proportional (E) terms, at each frequency point k, is the equation

$$\widetilde{F}(s_k) = \sum_{n=1}^{N} \frac{r_n}{s_k - p_n} + s_k E + d \approx F(s_k) \ , \tag{2.8}$$

with p_n as either real or one of a pair of complex conjugate poles, and r_n the corresponding residue term. Note that $\widetilde{F}(s)$ can also be expressed in equivalent pole-zero-gain form as

$$\widetilde{F}(s) = \frac{\widetilde{N}(s)}{\widetilde{D}(s)} = F_0 \frac{\prod_{m=1}^{M}(s - z_m)}{\prod_{n=1}^{N}(s - p_n)}, \tag{2.9}$$

where F_0 is a constant real gain, z_m represents one of the M zeros, and p_n represents one of the N poles.

When dealing with a strictly proper transfer function such that $M < N$, then when represented by partial fractions, the E and D terms in (2.8) are null and can be ignored.

As a ratio of polynomials, such a transfer function will have the form

$$\widetilde{F}(s) = \frac{\widetilde{N}(s)}{\widetilde{D}(s)} = \frac{b_0 + b_1 s + b_2 s^2 + ... + b_M s^M}{1 + a_1 s + ... + a_{N-1} s^{N-1} + a_N s^N}. \tag{2.10}$$

So, given K frequency response data points with frequency samples $s_k = j\omega_k$, (2.8) and (2.9) yield the following cost function minimization problem when trying to approximate $F(s_k)$:

$$\min \sum_{k=1}^{K} \left| F(s_k) - \frac{\widetilde{N}(s_k)}{\widetilde{D}(s_k)} \right|^2. \tag{2.11}$$

Equivalently,

$$\min \sum_{k=1}^{K} \frac{1}{\left|\widetilde{D}(s_k)\right|^2} \left| F(s_k)\widetilde{D}(s_k) - \widetilde{N}(s_k) \right|^2. \tag{2.12}$$

Note that (2.12) is non-linear and solvable within a desired margin of error using constrained optimization techniques. Such solutions, however, are computationally demanding when compared to those of linearized overdetermined least squares problems.

2.4 The Vector Fitting (VF) algorithm

The VF method [1] proposes a linearized method for identifying $F(s)$ in the least squares sense.

$$F(s) \cong \frac{\widetilde{N}(s)}{\widetilde{D}(s)} = \frac{\sum_{n=1}^{N} \frac{\hat{r}_n}{s-\bar{p}_n} + sE + d}{\sum_{n=1}^{N} \frac{\widetilde{r}_n}{s-\bar{p}_n} + 1}, \tag{2.13}$$

given that

$$\underset{s\to\infty}{Lim} \left(\sum_{n=1}^{N} \frac{\widetilde{r}_n}{s-\bar{p}_n} \right) = 0. \tag{2.14}$$

The VF algorithm then transforms (2.13) into

$$\sum_{n=1}^{N} \frac{\hat{r}_n}{s-\bar{p}_n} + sE + d - \left(\sum_{n=1}^{N} \frac{\widetilde{r}_n}{s-\bar{p}_n} \right) F(s) \cong F(s). \tag{2.15}$$

Given a sufficiently large number of frequency response data points for $F(s_k)$, the unknowns to be discovered are the residue terms $\hat{r}_n$, $\widetilde{r}_n$, the poles $\bar{p}_n$, and the direct and proportional terms, d and E, respectively. Solving for these is accomplished iteratively using a series of two overdetermined linear solutions by the least-squares method. These two main stages are known as the *pole relocation* and *residue identification* steps. A set of initial poles is selected to commence the procedure. At the end of each iteration, a new set of poles and residues are provided that can be used to test for convergence. The details of the formulation for these steps under VF is provided in [1].

The VF procedure from 2.13 can be recognized as a division of both numerator and denominator of (2.10) by the initialized poles, denoted as $D'(s)$ in the following expression

$$F(s) \cong \frac{N(s)/D'(s)}{D(s)/D'(s)}, \tag{2.16}$$

where $D'(s)$ may be represented by

$$D'(s) \;=\; \prod_{n=1}^{N} (s - p_n^{(i)}), \tag{2.17}$$

or as

$$D'(s) \;=\; b_0 + b_1 s + b_2 s^2 + ... + b_N s^N; \tag{2.18}$$

that is as a polynomial of order N with roots that correspond with the current iteration's poles ($p_n^{(i)}$).

Then, at each new iteration, the poles $D'(s)$ are re-initialized to hold values output from the previous iteration. When these poles are equal to the desired system poles $D(s)$ then the approximation has converged with the desired system transfer function $F(s)$.

The VF method can converge relatively quickly and accurately depending on the function to be fitted and the initial poles selected, however improvements have been made to this algorithm since its publication, specifically to resolve issues of ill-conditioning and convergence oscillation.

2.5 The Weighted Vector Fitting (WVF) algorithm

The Weighted Vector Fitting (WVF) technique involves the use of an inherent weighting term that updates after each fitting iteration [9, 10]. This weighting term enforces that the linearization step is more precise. For instance, in VF, the algorithm goes from the nonlinear expression of (2.12) to the linear expression (2.13) using

$$F(s) \cong \frac{\widetilde{N}(s)}{\widetilde{D}(s)} \tag{2.19}$$

$$\widetilde{N}(s) - \widetilde{D}(s)F(s) \cong 0. \tag{2.20}$$

However in WVF, the step taken by (2.20) is considered to be a source of error due to numerical inaccuracies inherent in the way the approximation is treated. Instead, a stricter approach is suggested in order to yield a more precise approximation for the basis functions, as follows, replacing (2.20) with:

$$\frac{\widetilde{N}(s)}{\widetilde{D}(s)} - F(s) \cong 0 \tag{2.21}$$

$$\frac{\widetilde{N}(s)}{\widetilde{D}(s)} - F(s)\frac{\widetilde{D}(s)}{\widetilde{D}(s)} \cong 0 \tag{2.22}$$

$$\frac{1}{\widetilde{D}(s)}\left[N(s) - \widetilde{F}(s)\widetilde{D}(s)\right] \cong 0. \tag{2.23}$$

Note that the effect of the term $\frac{1}{\widetilde{D}(s)}$ in (2.23) is analogous to that of $\frac{1}{\left|\widetilde{D}(s_k)\right|^2}$ from (2.12). Whereas in VF that term is ignored and set to unity, in WVF it is retained and updated iteratively.

That is to say, in WVF, going from the VF identity

$$F(s) \cong \frac{\sum_{n=1}^{N} \frac{\hat{r}_n}{s-\bar{p}_n} + sE + d}{\sum_{n=1}^{N} \frac{\widetilde{r}_n}{s-\bar{p}_n} + 1}, \tag{2.24}$$

the minimization problem then becomes

$$\min \left| \frac{1}{\sum_{n=1}^{N} \frac{\widetilde{r}_n}{s-\bar{p}_n} + 1} \left[\sum_{n=1}^{N} \frac{\hat{r}_n}{s-\bar{p}_n} + sE + d - \left(\sum_{n=1}^{N} \frac{\widetilde{r}_n}{s-\bar{p}_n} + 1 \right) F(s) \right] \right|. \tag{2.25}$$

For compactness of the expression, let the proportional and direct terms – which are only necessary for biproper and non-proper transfer functions – be replaced by the function

$$\widetilde{\alpha}(s) = sE + d. \tag{2.26}$$

In the iterative context of the fitting procedure, let i denote the i-th iteration, with $\widetilde{W}(s_k)$ and $\widetilde{D}(s_k)$ denote weighting terms for the current and next iteration such that

$$\widetilde{W}^{(i)}(s_k) = \sum_{n=1}^{N} \frac{\widetilde{r}_n^{(i-1)}}{s_k - \bar{p}_n^{(i-1)}} + 1 = \widetilde{D}^{(i-1)}(s_k). \tag{2.27}$$

Then, in WVF, going from the VF equation (2.13) the minimization problem becomes

$$\min \left| \frac{1}{\widetilde{W}^{(i)}(s_k)} \left[\sum_{n=1}^{N} \frac{\hat{r}_n^{(i)}}{s_k - \bar{p}_n^{(i)}} + \widetilde{\alpha}(s_k) - \widetilde{D}^{(i)}(s_k) F(s) \right] \right|. \tag{2.28}$$

In [9] this weighting technique has been demonstrated to alleviate problems of ill-conditioning and poor fitting that is otherwise present due to overemphasis on low frequency samples.

2.6 The Magnitude Vector Fitting (magVF) algorithm

Magnitude Vector Fitting is a more recent addition to the VF family tree that uses a symmetric partial fraction basis for the formulation of the overdetermined linear system equations to fit a magnitude-squared frequency response. The derivation presented in this section follows that of [11], in which the abbreviation magVF was first used.

Again, letting $F(s)$ be a Laplace transform of the impulse response $f(t)$ of a causal and stable LTI system. In product form, $F(s)$ can be represented by

$$F(s) = F_0 \frac{\prod_{m=1}^{M} (s - z_m)}{\prod_{n=1}^{N} (s - p_n)}, \tag{2.29}$$

where F_0 is a positive and real gain constant, z_m refers to each of the M zeros, and p_n refers to each of the N poles. For realizable bounded systems the order of the numerator (M) and denominator (N) are such that the system is either proper ($M = N$) or strictly proper ($M < N$).

Taking the Fourier Transform by resolving $F(s)$ on the imaginary axis, such that $F(s)|_{s=j\omega} = F(j\omega)$ and by complex number properties:

$$|F(j\omega)|^2 = F(j\omega)F^*(j\omega). \tag{2.30}$$

The magnitude-squared can also be expressed as

$$|F(j\omega)|^2 = F_0^2 \frac{\prod_{m=1}^{M} (j\omega - z_m)(-j\omega - z_m^*)}{\prod_{n=1}^{N} (j\omega - p_n)(-j\omega - p_n^*)}, \tag{2.31}$$

or by pulling out a negative sign, as

$$|F(j\omega)|^2 = (-1)^{(M-N)} F_0^2 \frac{\prod_{m=1}^{M} (j\omega - z_m)(j\omega + z_m^*)}{\prod_{n=1}^{N} (j\omega - p_n)(j\omega + p_n^*)} \tag{2.32}$$

Note the assumption that all poles and zeros are either purely real or present in complex-conjugate pairs. Provided that this is held true, by (2.32) it is evident that the magnitude-squared function is composed of poles and zeros in the left hand s-plane (LHP) as well as their symmetric counterparts in the right hand s-plane (RHP).

The problem thence assumes that there is a set $|F(j\omega_k)|^2$ of tabulated data of size K frequency-domain points for which an approximated transfer function that yields $|\widetilde{F}(j\omega_k)|^2 \backsimeq |F(j\omega_k)|^2$ is desired. Given the magnitude-squared form of (2.32), and then under the assumption that all poles and zeros are in the left hand s-plane – as is the case for minimum phase functions by definition – it is possible to eliminate the right-hand plane poles and zeros and, taking the square root of the F_0 term, to reduce the magnitude-squared to a simple magnitude approximation such that the non-squared magnitude response can be inferred.

$$|F(j\omega_k)| = F_0 \frac{\prod_{m=1}^{M} |j\omega_k - z_m|}{\prod_{n=1}^{N} |j\omega_k - p_n|} \backsimeq |\widetilde{F}(j\omega_k)| \tag{2.33}$$

Furthermore, (2.32) can also be represented in the following symmetrical partial-fractions form:

$$|F(j\omega_k)|^2 = r_0 + \sum_{n=1}^{N} \left(\frac{r_n}{j\omega_k - p_n} - \frac{r_n}{j\omega_k + p_n} \right), \tag{2.34}$$

noting that $r_0 = 0$ when $M < N$ and $r_0 = F_0^2$ when $M = N$.

Applying the standard VF method to the magnitude-squared function above leads to some problems with asymmetrically perturbed poles and residues. To counter this, the use of symmetric basis functions as a modification to VF has been suggested [11, 13] and provided in the following sections. Given that the overall algorithm is employed iteratively, in the ensuing discussion, the index i indicates the current iteration.

2.6.1 Step 1: Pole Relocation

Given a set of initial poles, that can be arbitrarily assigned and distributed within the bandwidth of our desired response at frequency points $j\omega_k$ of which there are K in total, the first step involves solving a LLS (Least Squares) problem of the form:

$$|\widetilde{N}(j\omega_k)|^2 - |F(j\omega_k)|^2 |\widetilde{D}(j\omega_k)|^2 \backsimeq 0 \tag{2.35}$$

Where

$$|\widetilde{N}(j\omega_k)|^2 = \sum_{n=1}^{N} \left(\frac{c_n}{j\omega_k - p_n^{(i)}} - \frac{c_n}{j\omega_k + p_n^{(i)}} \right) + d \tag{2.36}$$

$$|\widetilde{D}(j\omega_k)|^2 = \sum_{n=1}^{N} \left(\frac{\bar{c}_n}{j\omega_k - p_n^{(i)}} - \frac{\bar{c}_n}{j\omega_k + p_n^{(i)}} \right) + 1 \tag{2.37}$$

In terms of a linear system of equations, the following matrix notation can be employed

$$\mathbf{Ax} = \mathbf{b} \tag{2.38}$$

Then, for each frequency k of the tabulated data of size K let us assign the variable $g_{k,n}$ such

that, for the case when $p_n^{(i)}$ is a real pole of the ith iteration,

$$g_{k,n} = \frac{1}{j\omega_k - p_n^{(i)}} - \frac{1}{j\omega_k + p_n^{(i)}} \quad . \tag{2.39}$$

And for the case when $p_n^{(i)}$ and $p_{n+1}^{(i)}$ are complex conjugates:

$$g_{k,n} = \frac{1}{j\omega_k - p_n^{(i)}} - \frac{1}{j\omega_k + p_n^{(i)}} + \frac{1}{j\omega_k - p_n^{(i)*}} - \frac{1}{j\omega_k + p_n^{(i)*}} \tag{2.40}$$

$$g_{k,n+1} = \frac{j}{j\omega_k - p_n^{(i)}} - \frac{j}{j\omega_k + p_n^{(i)}} + \frac{j}{j\omega_k - p_n^{(i)*}} - \frac{j}{j\omega_k + p_n^{(i)*}}. \tag{2.41}$$

In [13] it is noted that the values of (2.39), (2.40), and (2.41) are real.

Now, constructing the kth row of the $\mathbf{A}$ matrix of linear Equation (2.38) as:

$$A_k = \begin{bmatrix} A_{k,1} & 1 & A_{k,2} \end{bmatrix} \tag{2.42}$$

With

$$A_{k,1} = \begin{bmatrix} g_{k,1} & \dots & g_{k,N} \end{bmatrix} \tag{2.43}$$

$$A_{k,2} = -|F(j\omega_k)|^2 \cdot \begin{bmatrix} g_{k,1} & \dots & g_{k,N} \end{bmatrix} \tag{2.44}$$

The solution vector, $\mathbf{x}$, corresponds with the following variables

$$\mathbf{x} = \begin{bmatrix} c_1 & \dots & c_N & d & \bar{c}_1 & \dots & \bar{c}_N \end{bmatrix}^T, \tag{2.45}$$

Note that this would be for the case of real poles. When the poles are complex conjugate pairs, as is the case for (2.40) and (2.41), then the coefficient terms will result in $c_m = c' + jc''$ and $c_{m+1} = c' - jc''$, and the corresponding variables in $\mathbf{x}$ will be c' and c''.

The $\mathbf{b}$ vector for the linear system of 2.38 is set as

$$\mathbf{b} = \begin{bmatrix} |F(j\omega_1)|^2 & \dots & |F(j\omega_K)|^2 \end{bmatrix}^T. \tag{2.46}$$

After constructing this overdetermined system of linear equations, it can be solved using a least-squares procedure.

Now, to find the new pole locations $p^{(i)}$, we modify the expression (2.37) such that

$$|D(s)|^2 = \sum_{n=1}^{N} \left(\frac{2\bar{c}_n p_n^{(i)}}{s^2 - (p_n^{(i)})^2} \right) + 1 \quad = \quad \frac{\prod_{n=1}^{N} (s^2 - \lambda_n)}{\prod_{n=1}^{N} (s^2 - (p_n^{(i)})^2)} \tag{2.47}$$

The zeros for this equation occur in opposite pairs since

$$\pm \sqrt{\lambda_n} = s \tag{2.48}$$

and the computation of λ_n can be accomplished using the same methodology described in [1] and re-derived for the magnitude squared case in [11]. That is:

$$\lambda_n = \text{eig}\{\widehat{\mathbf{A}} - \widehat{\mathbf{b}}\widehat{\mathbf{c}}^T\} \tag{2.49}$$

Where $\widehat{\mathbf{A}}$ is an N x N real block diagonal matrix, $\widehat{\mathbf{b}}$ is a column vector, and $\widehat{\mathbf{c}}$ is a row vector. Their entries are composed as follows:

- if p_n^2 is real, then the nth block of $\widehat{\mathbf{A}}$ is p_n^2, $\widehat{\mathbf{b}}_n = 1$, and $\widehat{\mathbf{c}}_n = 2\bar{c}_n p_n$
- else if $p_n^2 = p_n^{'} + jp_n^{''}$ and $p_n^2 = p_n^{'} - jp_n^{''}$ then the nth block of $\widehat{\mathbf{A}}$ is the 2 x 2 block

$$\widehat{\mathbf{A}}_n = \begin{bmatrix} p_n^{'} & p_n^{''} \\ -p_n^{''} & p_n^{'} \end{bmatrix} \tag{2.50}$$

  while $\widehat{\mathbf{b}}_n = 2$, $\widehat{\mathbf{b}}_{n+1} = 0$, $\widehat{\mathbf{c}}_n = \text{Re}\{2\bar{c}_n p_n\}$, and $\widehat{\mathbf{c}}_{n+1} = \text{Im}\{2\bar{c}_n p_n\}$

Since the matrix yielded by $\widehat{\mathbf{A}} - \widehat{\mathbf{b}}\widehat{\mathbf{c}}^T$ is real, then the eigenvalues found by (2.49) are either real or occur in complex conjugate pairs. Finding the relocated poles $p_n^{(i+1)}$ is done by taking the square root of each eigenvalue, such that

$$p_n^{(i+1)} = \pm\sqrt{\lambda_n}. \tag{2.51}$$

If the eigenvalue λ_n is real, then (2.51) implies a pair of poles that are real and symmetrical with respect to the imaginary axis. However, if the eigenvalues are complex conjugate pairs, then the resulting poles will be two symmetrical pairs of complex conjugates.

A problem arises when there are real negative eigenvalues, that is $\lambda_n < 0$. In this case, the new pole locations are entirely imaginary. These are called "unphysical pairs" in [11], which proposes a perturbation algorithm to avoid such poles. The perturbations occur after a predefined number of attempts to resolve the problem by changing the sign of the eigenvalues have failed to give suitable poles.

Algorithm 2.1 Algorithm for dealing with real negative eigenvalues during pole relocation (ie.$\lambda_n < 0$)

```
ASSIGN SMALL_EPSILON_RESIDUES;
ASSIGN SMALL_EPSILON_POLES;
ASSIGN MAX_ITERATIONS;
ASSIGN CONVERGENCE_CRITERA;
ASSIGN VF_METHOD_MAX;
i=0;
while ( (i≤MAX_ITERATIONS) && (CONVERGENCE_CRITERIA==False) )
    DO FIRST_PART_OF_POLE_RELOCATION_STEP;
    DO GET_EIGENVALUE_MATRIX;
    for m=1:size(EIGENVALUE_MATRIX)
        if (IMAG(EIG(m,m))==0 && (REAL(EIG(m,m))<0);
            THERE_EXISTS_NEG_EIGVALUE=true;
            if i<VF_METHOD_MAX && THERE_EXISTS_NEG_EIGVALUE,
                EIGENVALUEDIAGONALMATRIX(n,n) = -EIGENVALUEDIAGONALMATRIX(n
                    ,n);
            end
        end
    end

    DO REST_OF_POLE_RELOCATION_STEP
    DO RESIDUES_ID_STEP

    if UNPHYSICAL_PAIRS_OF_FRACTIONS && (i > VFMETHODMAX)
        Norder=Norder+2
        %the order grows, watch out!
        DO PERTURBATION SMALL_EPSILON_RESIDUES(c(n),c(n+1))
        DO PERTURBATION SMALL_EPSILON_POLES(p(n),p(n+1))
    end
    i = i+1;
end
if (i>MAX_ITERATIONS)
    'FAILURE: DIVERGENCE'
    return 0 %FAILURE CONDITION
end
if (DO_TEST(CONVERGENCE_CRITERIA)==1)
    'SUCCESS: CONVERGENCE'
    return 1 % SUCCESS CONDITION
end
'LOGIC ERROR'
return -1 % LOGIC ERROR
```

2.6.2 Step 2: Residue Identification

After the relocation of the poles, the algorithm continues with the residue identification step, which involves solving another overdetermined least squares problem derived from

(2.34). The basic equation for this step is

$$|F(j\omega_k)|^2 = r_0 + \sum_{n=1}^{N} \left(\frac{r_n}{j\omega_k - p_n^{(i+1)}} - \frac{r_n}{j\omega_k + p_n^{(i+1)}} \right) \tag{2.52}$$

Here the unknown residues r_n are solved again using the basic structure

$$\mathbf{Ax} = \mathbf{b} \tag{2.53}$$

Similar to the formulation of the $\mathbf{A}$ matrix during the pole relocation step, one can assign a temporary variable $g_{k,n}$, this time using the relocated pole $p_n^{(i+1)}$.

$$g_{k,n} = \frac{1}{j\omega_k - p_n^{(i+1)}} - \frac{1}{j\omega_k + p_n^{(i+1)}}. \tag{2.54}$$

For the case when $p_n^{(i+1)}$ and $p_{n+1}^{(i+1)}$ are complex conjugates:

$$g_{k,n} = \frac{1}{j\omega_k - p_n^{(i+1)}} - \frac{1}{j\omega_k + p_n^{(i+1)}} + \frac{1}{j\omega_k - p_n^{(i+1)*}} - \frac{1}{j\omega_k + p_n^{(i+1)*}} \tag{2.55}$$

and

$$g_{k,n+1} = \frac{j}{j\omega_k - p_n^{(i+1)}} - \frac{j}{j\omega_k + p_n^{(i+1)}} + \frac{j}{j\omega_k - p_n^{(i+1)*}} - \frac{j}{j\omega_k + p_n^{(i+1)*}}. \tag{2.56}$$

Next, constructing the kth row of the $\mathbf{A}$ matrix of (2.53) as:

$$A_k = \begin{bmatrix} 1 & g_{k,1} & \dots & g_{k,N} \end{bmatrix}. \tag{2.57}$$

The solution vector, $\mathbf{x}$, corresponds with the residues

$$\mathbf{x} = \begin{bmatrix} r_0 & r_1 & \dots & r_N \end{bmatrix}^T. \tag{2.58}$$

The $\mathbf{b}$ vector is set to

$$\mathbf{b} = \begin{bmatrix} |F(j\omega_1)|^2 & \dots & |F(j\omega_K)|^2 \end{bmatrix}^T. \tag{2.59}$$

Now, (2.53) can be solved for the unknowns in $\mathbf{x}$, giving the square of the DC gain and the residues of the magnitude square approximation.

2.6.2.1 Disciplined Convex Programming (DCP) to ensure non-negative definite magnitude-squared function

When using (2.34) to construct the approximated magnitude-squared response, magVF may return negative values at certain frequencies, particularly those where the magnitude has dropped very close to zero, and numeric artifacts of the least-squared residues solutions become more apparent. Obviously, negative values are not realistic for a magnitude-squared response. In [11] Disciplined Convex Programming [21] is used to optimize the election of residues, to ensure that the resulting magnitude squared approximation returned by (2.34) remains non-negative definite, such that, for all frequency points ω_k,

$$|F(j\omega_k)|^2_{approx} \geq= 0, \tag{2.60}$$

and

$$r_0 \geq= 0. \tag{2.61}$$

Optimization techniques can be computationally expensive, and so a procedure for introducing this procedure only as required is shown in Algorithm 2.2, where `SERA` represents the input poles, `SERA'` represents the output (relocated) poles, and `opts.OPTIMIZE_RESIDUES` is a boolean that, if true, sets the magVF function to perform the optimization.

Algorithm 2.2 Algorithm for applying residues optimization as required

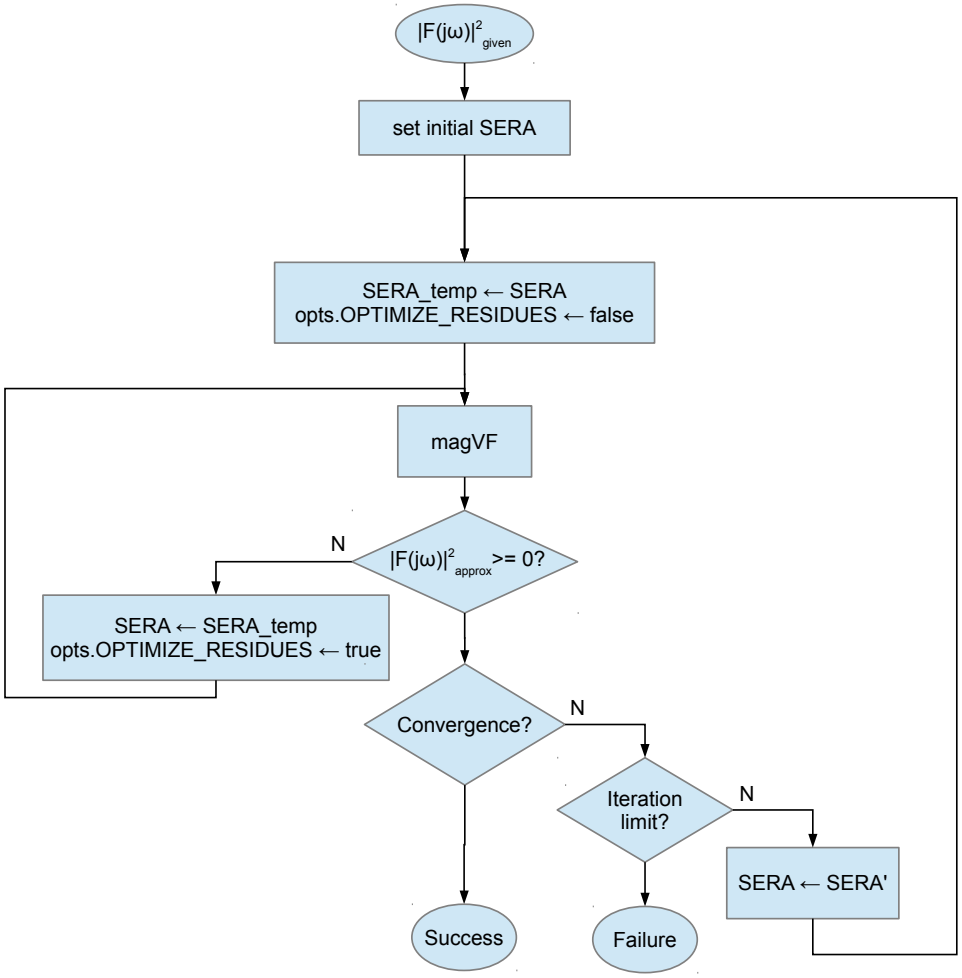

In that algorithm, initially the variable `opts.OPTIMIZE_RESIDUES` is set to false, and only after testing to see if the approximated magnitude-squared response is negative at some ω_k will it then be set to true. Then the last iteration will recommence by reloading the saved input poles (discarding the `SERA'` output from most recent iteration), and making another call to the magVF fitter again with the optimization flag set. Note that it is prudent to perform an additional logic test just before the test for non-negative definiteness, to ensure that if the `opts.OPTIMIZE_RESIDUES` is true (and hence optimization was performed in the last call to magVF), and even if the non-negative definiteness property is violated again, the algorithm could continue further, instead of being caught in an infinite loop condition.

The relevant MATLAB code using the `cvx` software package [22] is given in Algorithm 2.3, where `A`, `x`, and `b` are the internal $\mathbf{Ax} = \mathbf{b}$ least squares overdetermined system variables as defined using (2.57), (2.58), (2.59). The variable `offs` is set based on the relative order of the numerator and denominator, and determines whether an additional constraint that r_0

from 2.52 is also non-negative is required.

Algorithm 2.3 MATLAB procedure for optimizing residues based on non-negative definiteness property

```
if (opts.OPTIMIZE_RESIDUES)
    Bz=zeros(size(B));
    cvx_begin quiet
        variable x(Norder+offs) complex;
        minimize( norm(A*x-B,2) );
        subject to
            real(A*x) ≥ Bz;
            if (opts.asympflag>1)
                real(x(Norder+offs)) ≥ 0; % this corresponds with constant
                    part, r_0
            end
    cvx_end
else
    x=(A)\B;    % LLS solver will be used
end
```

Thus, if the boolean variable `opts.OPTIMIZE_RESIDUES` is true, the `cvx` algorithm is run, otherwise the usual linear least-squares (LLS) solution is employed.

CHAPTER 3

MODIFICATIONS TO MAGNITUDE VECTOR FITTING

3.1 Weighted magVF (WmagVF) formulation

In this section, the formulation of a proposed Weighted Magnitude Vector Fitting (WmagVF) algorithm is demonstrated. The motivation and methodology behind this algorithm is analogous to that of WVF, as presented earlier, in Section 2.5. The fundamental difference comes out of the type of basis functions employed in magVF versus regular VF.

Taking the symmetric basis functions in the numerator and denominator for the case where $M < N$,

$$|F(s)|^2 \cong \frac{\sum_{n=1}^{N}\left(\frac{\hat{c}_n}{s-\bar{p}_n}-\frac{\hat{c}_n}{s+\bar{p}_n}\right)}{\sum_{n=1}^{N}\left(\frac{\tilde{c}_n}{s-\bar{p}_n}-\frac{\tilde{c}_n}{s+\bar{p}_n}\right)+1}. \tag{3.1}$$

Where,

$$|F(s)|^2 \cong \frac{|\widetilde{N}(s)|^2}{|\widetilde{D}(s)|^2}. \tag{3.2}$$

Then,

$$\frac{|\widetilde{N}(s)|^2}{|\widetilde{D}(s)|^2} - |F(s)|^2 \cong 0 \tag{3.3}$$

$$\frac{|\widetilde{N}(s)|^2}{|\widetilde{D}(s)|^2} - |F(s)|^2\frac{|\widetilde{D}(s)|^2}{|\widetilde{D}(s)|^2} \cong 0 \tag{3.4}$$

$$\frac{1}{|\widetilde{D}(s)|^2}\left(|\widetilde{N}(s)|^2 - |F(s)|^2|\widetilde{D}(s)|^2\right) \cong 0 \tag{3.5}$$

Now using an analogous approach as in WVF, including a weighting factor $\widetilde{W}(j\omega_k)$ that is composed of $|\widetilde{D}(j\omega_k)|^2$ from the previous iteration

$$\widetilde{W}^{(i)}(j\omega_k) \;=\; \sum_{n=1}^{N}\left(\frac{\tilde{c}_n^{(i-1)}}{j\omega_k-\bar{p}_n^{(i-1)}}-\frac{\tilde{c}_n^{(i-1)}}{j\omega_k+\bar{p}_n^{(i-1)}}\right)+1\ , \tag{3.6}$$

or more simply stated as

$$\widetilde{W}^{(i)}(j\omega_k) \;=\; |\widetilde{D}^{(i-1)}(j\omega_k)|^2 \;, \tag{3.7}$$

and

$$\frac{1}{\widetilde{W}^{(i)}(j\omega_k)}\left[|\widetilde{N}^{(i)}(j\omega_k)|^2 - |F(j\omega_k)|^2|\widetilde{D}^{(i)}(j\omega_k)|^2\right] \backsimeq 0. \tag{3.8}$$

For the first iteration let $\widetilde{W}^{(i)}(j\omega_k) = 1$ for all k. Subsequently, at the end of each iteration compute the next weighting term from $|\widetilde{D}^{(i)}(j\omega_k)|^2$, as $\widetilde{W}^{(i+1)}(j\omega_k)$. This value is used at each iteration to scale the k-th row of elements of equations represented by matrix $\mathbf{A}$ and right-hand side vector $\mathbf{b}$ from the equation $\mathbf{Ax} = \mathbf{b}$ in the pole relocation step prior to solving for the new poles. This study proposes that in doing so, the convergence characteristics with respect to the precision of the solution can be improved for certain transfer functions.

3.2 Input Pole Modification

Input Pole Modification is a simple preliminary intervention that can be included in the VF and magVF based fitting procedure. Since the modal propagation functions for transmission lines and cables have generally smooth magnitude responses, [4] suggests it is best to use real and logarithmically spaced values for their starting poles. In this vein, two new pole modification schemes were devised. Given an input set of poles (SERA), the algorithm for these is expressed using Algorithm 3.1.

Algorithm 3.1 Pole modifications based on parameter `opts.poleMod` used in W/VF and W/magVF fitters

```
if (opts.poleMod==1)
    SERA=real(SERA);
elseif (opts.poleMod==2)
    SERA=-abs(SERA);
end
```

The variable `opts.poleMod` is one of the possible parameters to the W/magVF and W/VF fitters, and the input poles (`SERA`) are modified according to how this parameter is set. If the `opts.poleMod` variable is set as either `1` or `2`, then the input poles will either be stripped of their imaginary parts, or be replaced by their negative magnitudes, respectively. This way, all the input poles for the fitting iterations will be real and stable, lending themselves well to approximating smooth magnitude responses, under the pretexts of reducing the burden of unnecessary complex poles on the final solution.

3.3 Summary of proposed modifications to magVF

To reiterate, the two major modifications proposed to the magVF algorithm are:

1. an iteratively updating Weighting method analogous to that used in WVF, and
2. an Input Pole Modification step that biases the input poles based on the type of output expected.

Figure 3.1 provides a block diagram comparison of the original magVF function before and after inclusion of these new modifications.

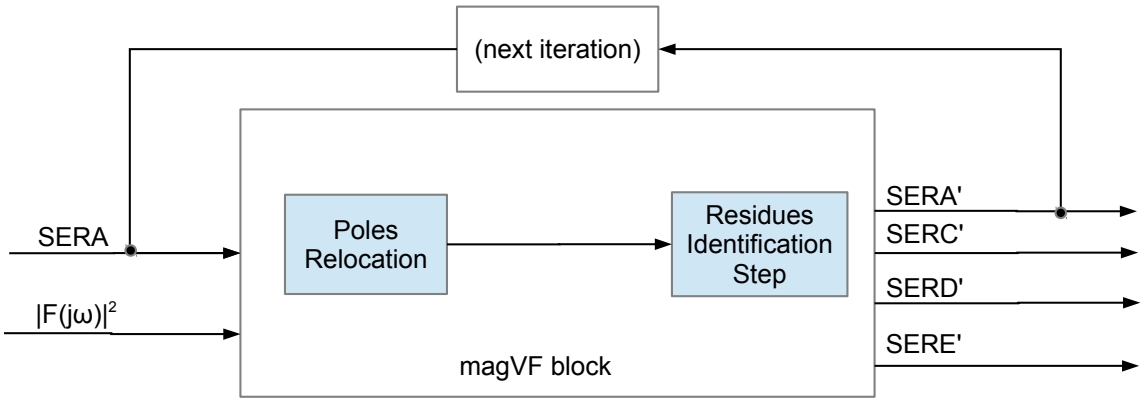

(a) magVF

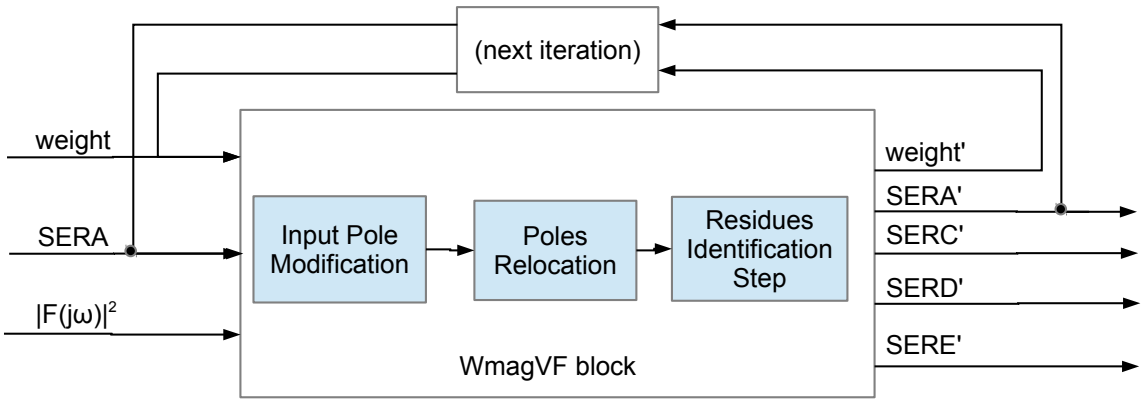

(b) WmagVF (with input pole modification)

Figure 3.1: Block diagram representations of original magVF and proposed WmagVF (with pole modification)

This type of graphical representation shows how the next iteration input poles and weights (`SERA` and `weight`) are derived from the output of the previous iteration. Furthermore, the output poles, residues, direct, and proportional terms (`SERA'`, `SERC'`, `SERD'`, and `SERE'`, respectively) can be then be used to construct the approximated magnitude-squared response $|F(j\omega_k)|^2_{approx}$ using (2.52). This can be compared with the magnitude-squared input for convergence, or reduced to magnitude and phase using techniques and assumptions that may

allow it. These techniques are external to the actual W/magVF algorithms, and are not shown here, but are discussed later, specifically as they relate to minimum-phase systems and modal propagation functions.

CHAPTER 4

TESTING IMPLEMENTED ALGORITHMS

4.1 Overview

In order to observe the functionality of the W/VF and W/magVF fitter implementations, a series of tests were conducted against various defined minimum-phase transfer functions. The functions included those with the following characteristics:

- A first order low pass filter, with and without a delay
- A biproper function, where the order of the numerator is equal to the order of the denominator, using different offset settings in the fitters
- functions with poles of higher multiplicity (repeated poles)

Also, some tests were run with mixed-phase systems (i.e., with zeros on either side of the imaginary axis in the Laplace domain), to see how they might be treated with W/magVF.

The goal of these tests was to become aware of the practical limitations of the algorithms and methods. The methodology, results, and discussion for these tests is presented in the following sections of this thesis.

4.2 Methodology

4.2.1 Creating arbitrary responses

The test procedure consisted of first constructing the impulse frequency responses of transfer functions based on the specified poles, zeros, gain, and a delay. The following algorithm was employed to achieved this.

Algorithm 4.1 MATLAB procedure for generating the frequency response based on poles, zeros, gain, and delay

```
function [fResponse] = frequencyResponseGeneratorPZForm(frequencyVector,
   thePoles,theZeros,theGain,theDelay)

    % INPUT
    % frequencyVector is a vector of frequency points, ...
    % in rad/s, something like logspace(-2,8,80)
    % thePoles and theZeros are both vectors, using the convention that ...
    % negative implies left-hand s-plane
    % theGain and theDelay are real values, scalars

    % OUTPUT
    % returns fResponse, which is the complex frequency response to be
       fitted, as
    % defined at each frequency point of frequencyVector


    s = sqrt(-1)*frequencyVector;  % s=jw

    num=1;
    denom=1;
    for e = 1:length(theZeros),
        num = num .* (s-theZeros(e));
    end

    for e = 1:length(thePoles),
        denom = denom .* (s-thePoles(e));
    end

    fResponse = ((exp(-s*theDelay)).*(theGain * (num./ denom))).';

return
```

An alternate method was also used to allow for the specifications based on residues, poles, and delay.

Algorithm 4.2 MATLAB procedure for generating the frequency response based on poles, residues, direct and proportional terms and delays

```
function [fResponse] = frequencyResponseGeneratorPRForm(frequencyVector,
    SERA,SERC,SERD,SERE,theDelay)

    % INPUT
    % frequencyVector is a vector of frequency points, something like
       logspace(-2,8,80)
    %


    % OUTPUT
    % returns f, which is the complex frequency response to be fitted, as
    % defined at each frequency point of frequencyVector


    s = sqrt(-1)*frequencyVector;

    num=1;
    denom=1;

    if length(SERA) ~= length(SERC)
        'this is not going to work!, SERA and SERC need to be the same size
           !'
    end
    for sn = 1:length(s),
        fResponse(sn) = SERD + SERE*s(sn);
        for m = 1:length(SERA),
            fResponse(sn) = fResponse(sn) + SERC(m)/(s(sn)-SERA(m));
        end
    end

    fResponse = exp(-s*theDelay).*fResponse.';
return
```

Then the magVF and VF algorithms – with and without weighting – were validated against the derived responses to see how they performed. The fitted results were collated and analyzed, and a summary of the findings is presented in the following.

4.2.2 Figures of merit employed

The equations for figures of merit employed for this and later tests, are as follows:

$$\epsilon_{abs_1}(k) = \left| \left| \widetilde{F}(s_k) \right| - |F(s_k)| \right| \tag{4.1}$$

$$\epsilon_{abs_2}(k) = \left| \widetilde{F}(s_k) - F(s_k) \right| \tag{4.2}$$

$$MAE_1 = maxerr_1 = max\left\{\epsilon_{abs_1}(k)\right\} \tag{4.3}$$

$$MAE_2 = maxerr_2 = max\left\{\epsilon_{abs_2}(k)\right\} \tag{4.4}$$

$$RMSE_1 = rmserr_1 = \sqrt{\frac{1}{K}\sum_{k=1}^{K}\epsilon_{abs_1}^2(k)} \tag{4.5}$$

$$RMSE_2 = rmserr_2 = \sqrt{\frac{1}{K}\sum_{k=1}^{K}\epsilon_{abs_2}^2(k)} \tag{4.6}$$

4.2.3 Iterative method for fitting based on approximation order and $RMSE_2$

For these tests, the approximation order was increased iteratively, with the goal of arriving below an $RMSE_2$ threshold of 1E-9 rad/s. This convergence criteria was chosen to demonstrate the exactness of the approximations being derived for low-order systems. A more practical limit may be less stringent under conditions where one is trying to fit higher order systems with fewer frequency response data points, as shall be demonstrated later when fitting transmission line and cable data.

The initial fit was attempted with 1 pole, for 30 iterations. The best result of those 30 iterations was tested against the $RMSE_2$ threshold, and if the convergence criteria was not yet met, the order was increased by one and the fitter was run for another 30 iterations. The maximum order was set to 20, such that a maximum of 20 poles would be fitted. Given that the approximation was based on 80 frequency samples logarithmically spaced, it was appropriate to choose this as the limit to ensure that the least-squares fitting remained well-conditioned. It is useful to mention here that magVF and VF use basis functions that contain approximately twice as many variables as there are poles. Thus, to remain over-determined it is justified to limit the order (ie. the number of poles) of the fitting to 1/4 of the frequency samples available. If the fitter was not successful after trying with 20 poles, then the iterations were stopped, and the fit using that particular method was deemed a failure.

4.3 Results

4.3.1 First order LPF with and without delay

A first order low-pass filter type transfer function was defined with the following characteristics:

Test case #	10
Given Poles	-1E3 rad/s
Given Zeros	None
Given DC Gain	1E3
Given Delay	0s

Table 4.1: First order LPF defined for Case 10

The fitting results are shown in Fig. (4.1).

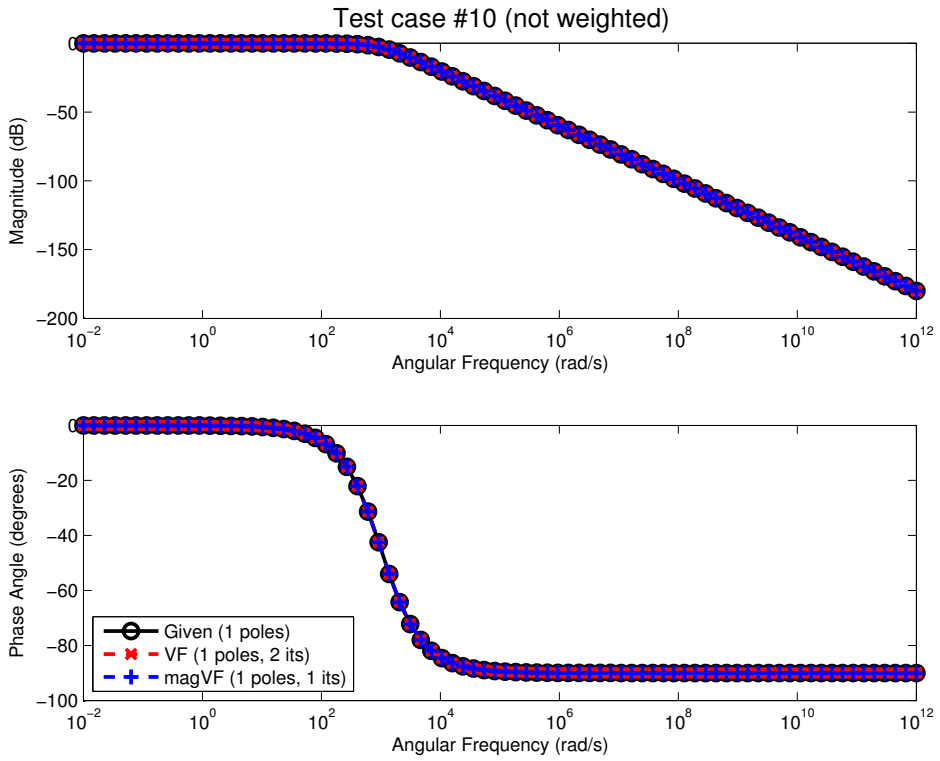

(a) without weighting

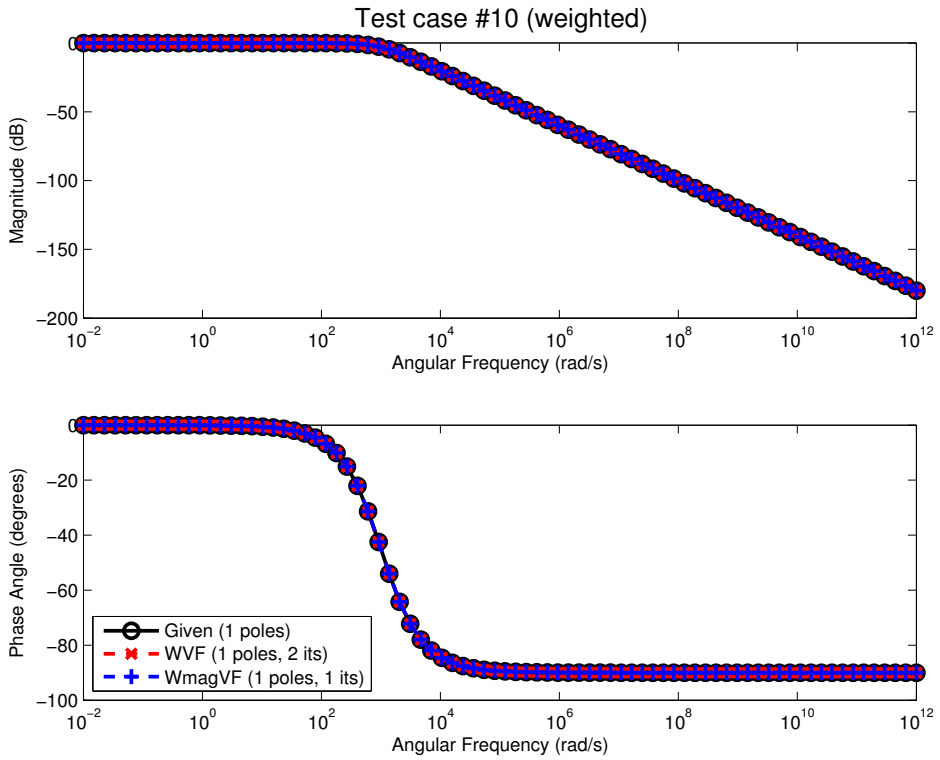

(b) with weighting

Figure 4.1: First order low pass filter as per Table (4.1)

As can be seen from the results, the fit was successful using the same approximation order as that of the original system (ie., same number of poles). The resulting values were exact. Weighting appeared to improve the convergence slightly for both types of fitters.

4.3.1.1 Effect of Delay

A test was run to see what the effect of a time delay would be on the fitters. Such examples are important for understanding the fitting of transmission lines and cable propagation modes.

A first order transfer function was defined as for Test case #10, except now a delay of 3 ms was included. The new parameters were assigned case #12 , as shown in Table (4.2) and results are shown in Fig. (4.2).

Test case #	12
Given Poles	-1E3 rad/s
Given Zeros	None
Given DC Gain	1E3
Given Delay	3E-3 s

Table 4.2: First order LPF defined for Case 12

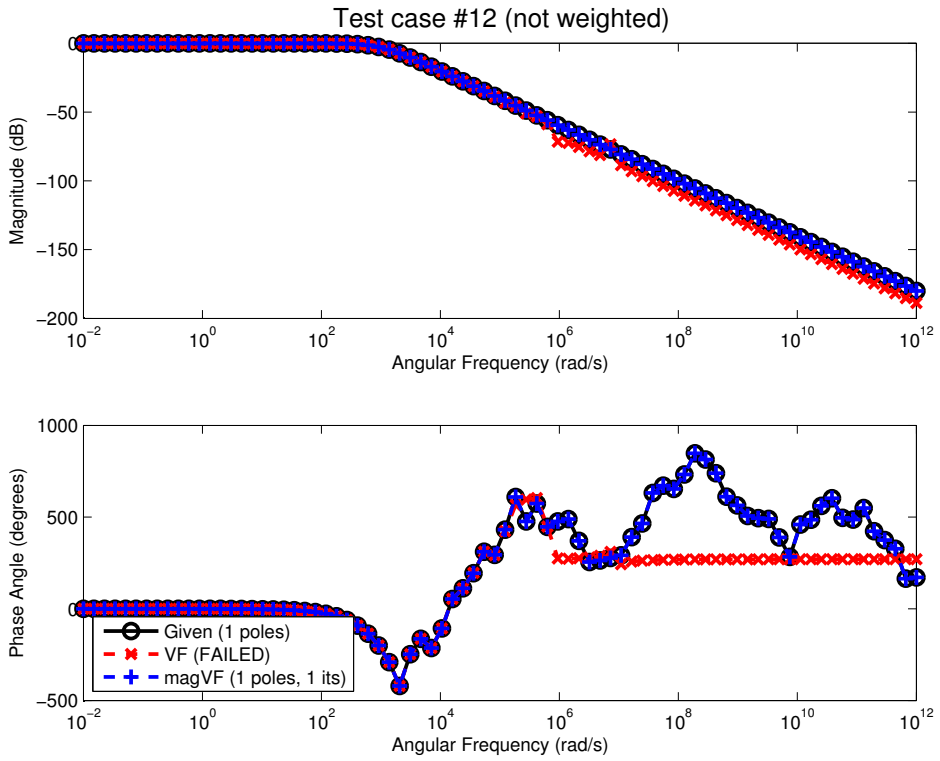

(a) without weighting

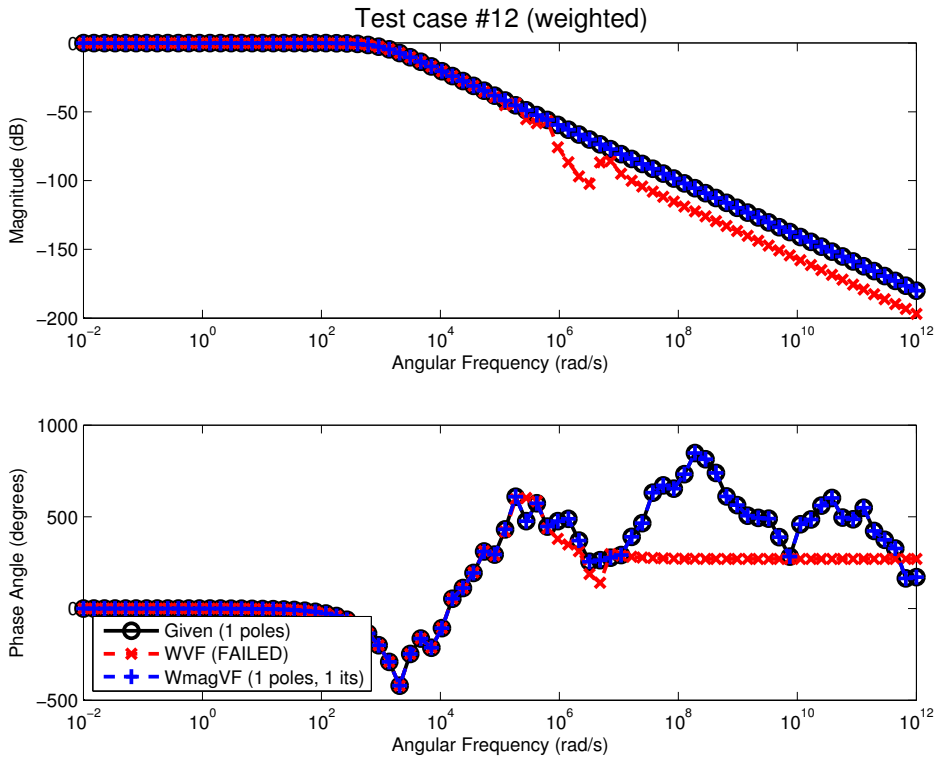

(b) with weighting

Figure 4.2: Delayed first order LPF

Note that in the Fig. 4.2 the phase responses do not roll-off smoothly as expected analytically, due to numerical artifacts in the phase computations of complex numbers that are close to the origin (low magnitudes). In such cases, the phase angle returned by functions such as `atan2` or `angle` in numerical platforms such as MATLAB are poorly defined, and hence when a delay is subtracted, this behaviour becomes more problematic.

Nonetheless, the approximations using W/magVF were exactly mirroring that of the desired response. The W/magVF methods were successful in extracting the delay after fitting the magnitude-squared response. Opposingly, W/VF failed in this regard, namely because the initial fit incorporates the delay and ends up corrupting the result since such delays are not accounted for in the internal basis function of the least squares problem. This is the type of issue which is typical encountered during transmission line and cable approximation.

The W/VF method fits the imaginary and real parts of the response as separate components, maintaining the delay as a part of the problem, while W/magVF fits the magnitude-squared response directly, coupling the imaginary and real parts and removing the effect of delays by virtue of taking the product of the response with its complex conjugate when performing the fit.

Thus, given a complex response in the Fourier domain, which is composed of an undelayed component $H'_m(j\omega)$ and the time delay which is represented by $e^{-j\omega\tau_m}$, such that

$$H_m(j\omega) = H'_m(j\omega)e^{-j\omega\tau_m}, \tag{4.7}$$

then

$$|H_m(j\omega)|^2 = H_m(j\omega)H^*_m(j\omega) = H'_m(j\omega)\left(H'_m(j\omega)\right)^* e^{-j\omega\tau_m}e^{j\omega\tau_m}. \tag{4.8}$$

Hence the delay τ_m gets cancelled in the squared-magnitude response, and so

$$|H_m(j\omega)|^2 = H'_m(j\omega)\left(H'_m(j\omega)\right)^*. \tag{4.9}$$

Therefore, there are significant differences in the way delays are dealt with when using the magnitude-squared response. For magVF, the delays are removed by virtue of the magnitude-squaring, so that they do not affect the fitting, and can be solved for after fitting the magnitude-squared function.

Conversely, in VF, iterative methods must be employed to find the delay before a successful fit can be finally achieved, as demonstrated in [19, 20, 9, 23, 10].

It is, therefore, unsurprising that magVF would be more successful during these tests. This test is inherently biased toward magVF since there is no *a priori* compensation algorithm included in the VF fitting. Such an algorithm for VF would involve significant iterative procedures, as is demonstrated in Chapter 5, when fitting actual modal propagation functions.

4.3.2 Fitting biproper functions (relative order = 0)

Tests were conducted to see how the fitters faired when trying to fit biproper functions. Biproper functions are those which have the same number of finite poles as zeros[1]. Transmission line and cables propagation functions are assumed to be strictly proper. Nevertheless, it is useful to investigate the fitting of biproper functions to see what effect the changing the relevant fitter setting (`asympflag`) is.

A two-pole, two-zero LPF was defined as follows, using entirely real poles.

Test case #	70, 71
Given Poles	-10E7, -10E6 rad/s
Given Zeros	-10E8, -10E9 rad/s
Given DC Gain	1E-4
Given Delay	0 s

Table 4.3: Second order biproper LPF defined for Case 70, 71

The fitters were run, using the fitters set to for strictly proper functions ($asympflag = 1$).

[1]Strictly proper functions are those which have more poles than zeros, and these are guaranteed to be stable, since the overall high frequency magnitude response is monotonically decreasing due to the dominance of the poles.

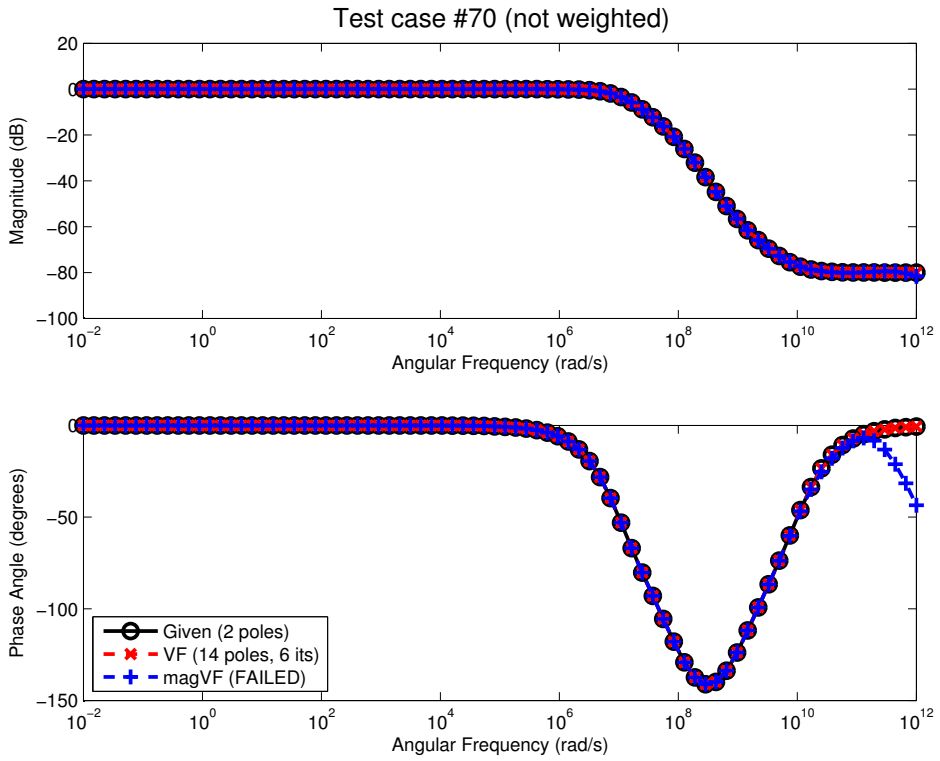

(a) without weighting

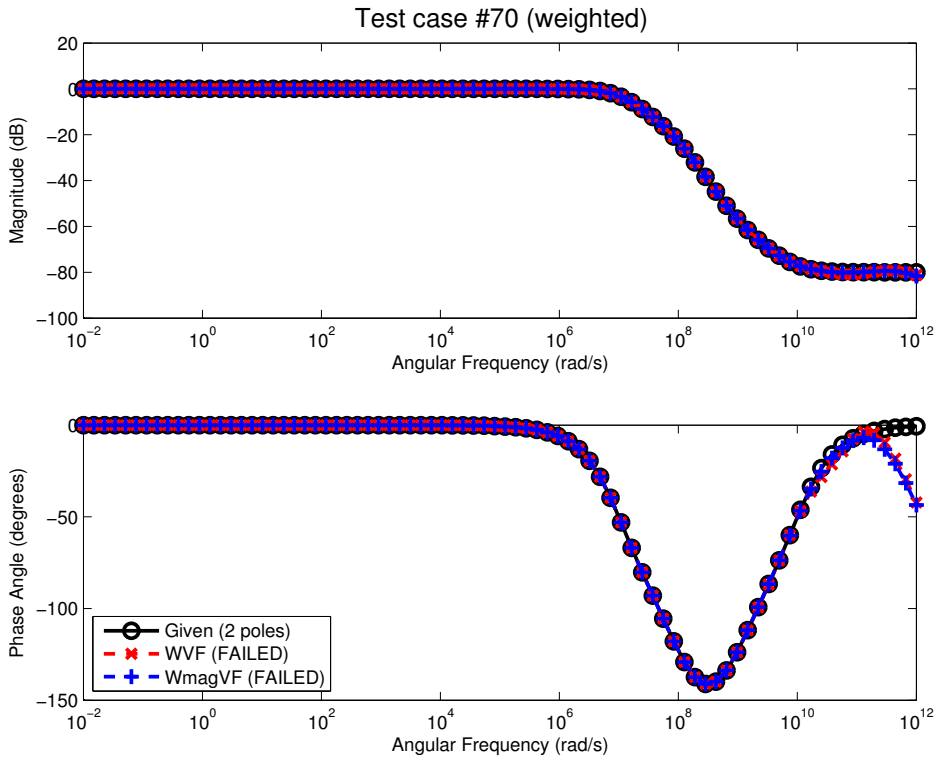

(b) with weighting

Figure 4.3: Biproper function fitted using strictly proper settings, $asympflag = 1$

The results of Fig. (4.3) show that high frequency fitting demonstrated decayed accuracy when using strictly proper settings, failing both fitters in the weighted case, and converging with VF but requiring 14 poles to do so.

Alternatively, it was possible to fit the biproper function quite well using the appropriate settings when running the fitters, as shown in Fig. (4.4).

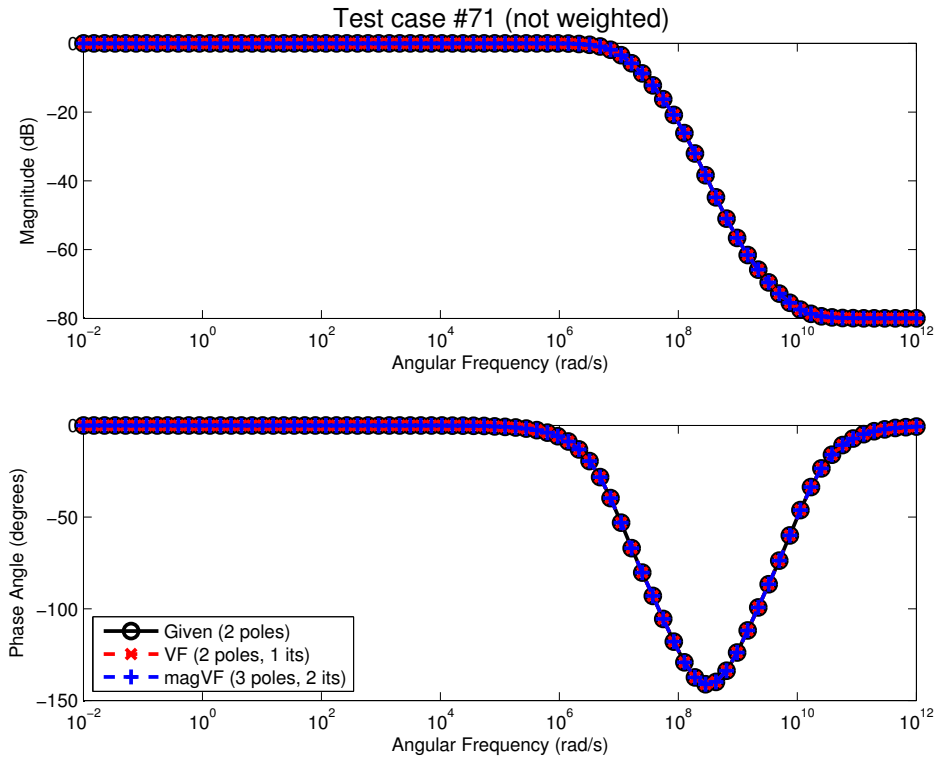

(a) without weighting

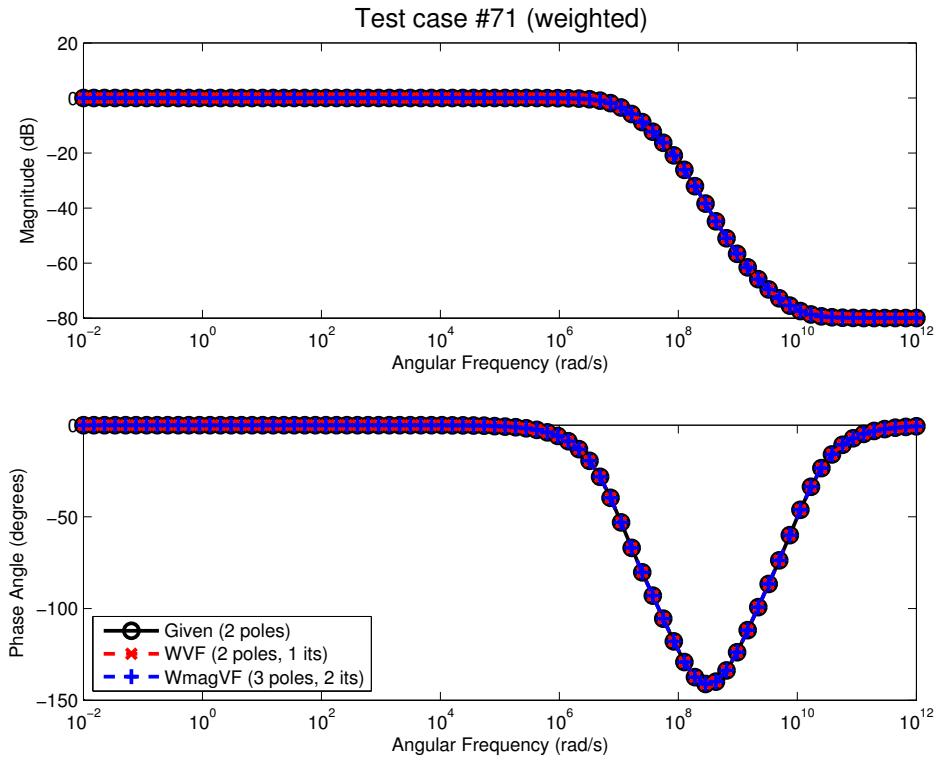

(b) with weighting

Figure 4.4: Biproper transfer function test case (Case #71), using biproper settings in the fitters, $asympflag = 2$

Although the results may not play a big role in the fitting of cables and transmission line transfer functions, it was useful to discover how such function fitting is affected by the choice of parameters. When trying to fit responses with unknown relative order it could help to modify this flag if the fit appears unsuccessful after initial trials.

4.3.3 Poles of higher multiplicity

It has been noted in previous works that VF has demonstrated problems with poles of higher multiplicity [24]. This issue was investigated here, to determine what the effect of using magVF (and weighting) is on transfer functions which contain poles with multiplicity greater than unity. A system was constructed using two repeated real poles and one real zero, as shown in Table (4.4).

Test case #	90
Given Poles	-1E6, -1E6 rad/s
Given Zeros	-1E3 rad/s
Given DC Gain	1E9
Given Delay	0 s

Table 4.4: Real repeated poles, test case #90

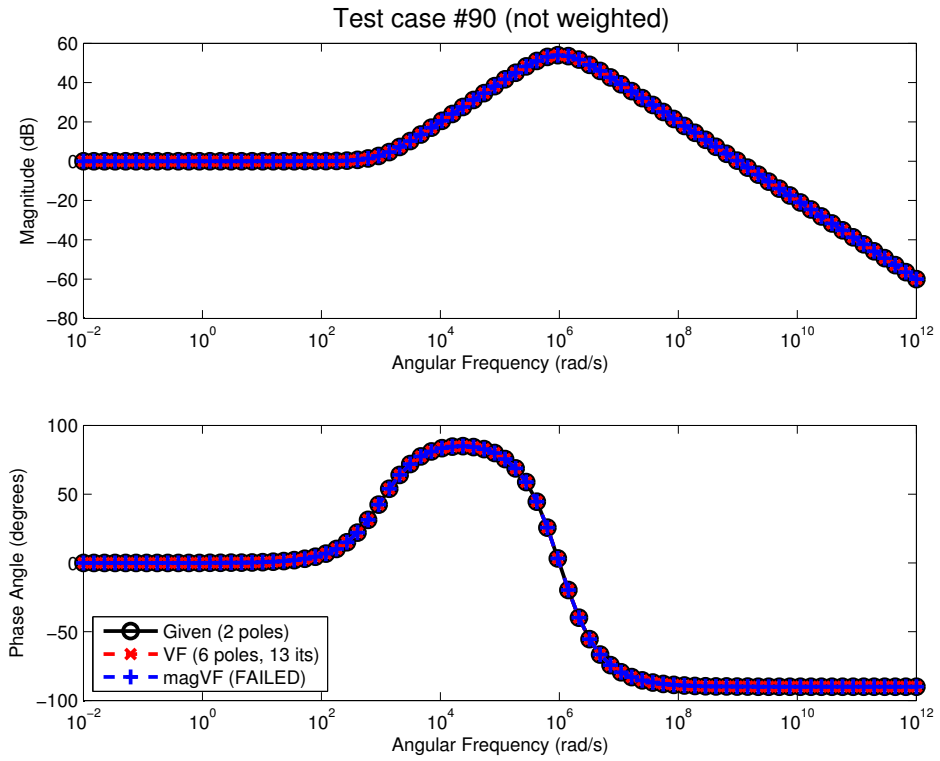

(a) without weighting

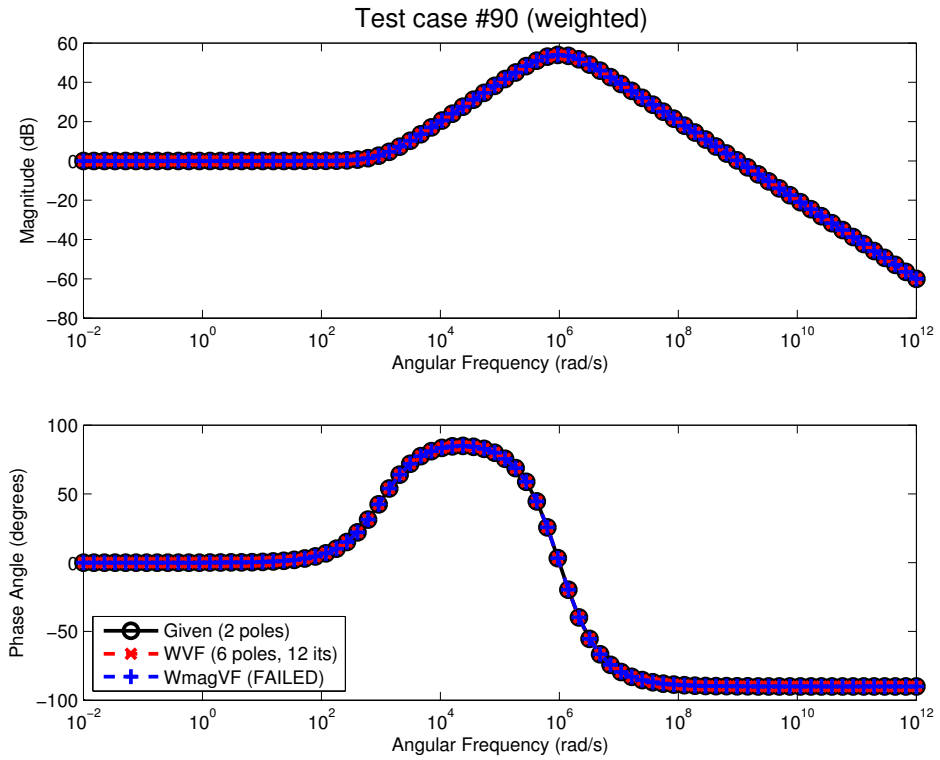

(b) with weighting

Figure 4.5: Repeated poles test case

As can be seen in Fig. (4.5), W/VF required 6 poles to achieve a suitable convergence $RMSE_2$ for a given 2 repeated pole case. Unfortunately, magVF did not achieved convergence even after including 20 poles, although the results appear close. Nevertheless, VF required 3 times as many poles as the actual system, while magVF used the maximum allowed and still did not achieve results below the desired convergence $RMSE_2$ of 1E-9 rad/s. By visual inspection, the results look close, but numerically the required error was not met. This indicates that both types of fitters (with and without weighting) require over-approximation of this repeated poles case.

Another case was tried, using two pairs of repeated complex poles, and two repeated real zeros (case #91).

Test case #	91
Given Poles	-1E6+1E6j, -1E6+1E6j -1E6-1E6j, -1E6-1E6j rad/s
Given Zeros	-1E3, -1E3 rad/s
Given DC Gain	4E18
Given Delay	0 s

Table 4.5: Complex repeated poles, test case #91

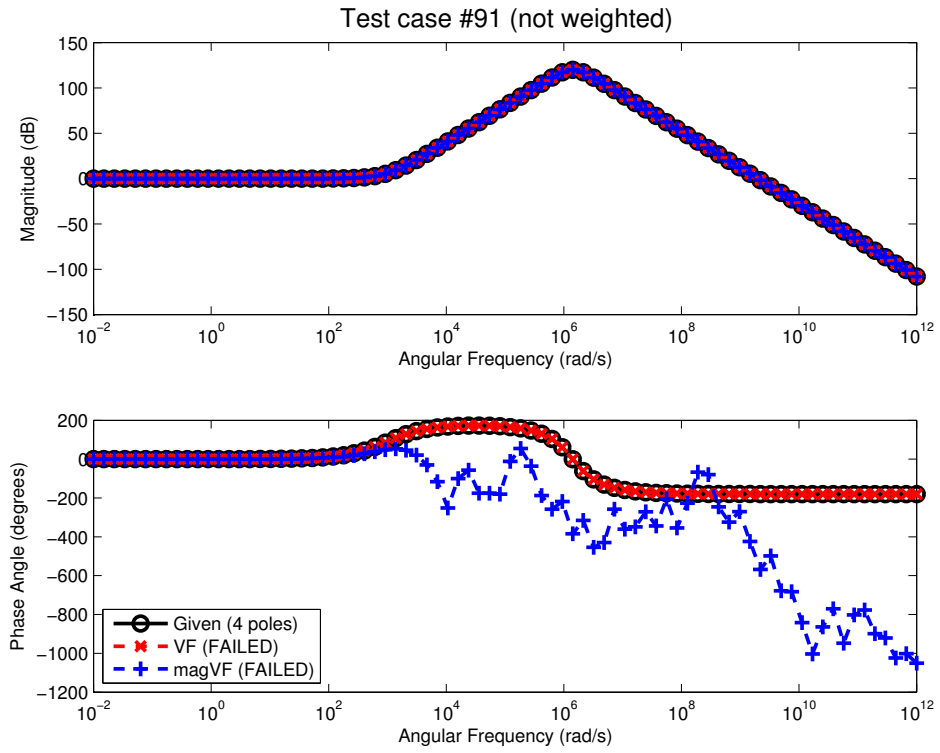

(a) without weighting

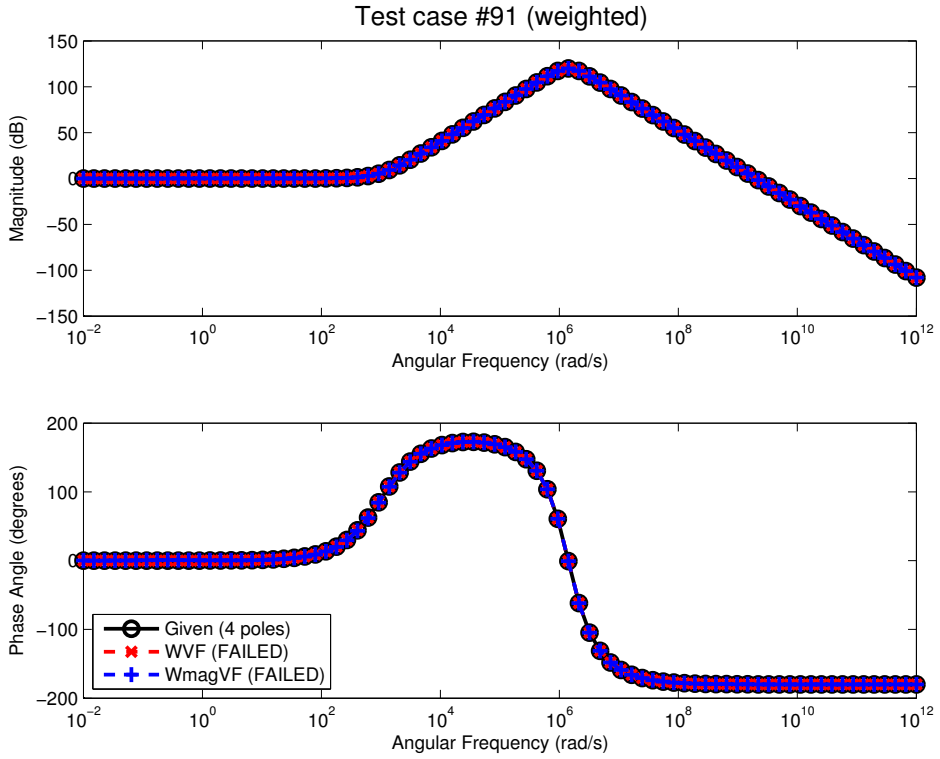

(b) with weighting

Figure 4.6: Repeated poles test case #91. All fitters fail, but weighting makes evident improvement for magVF.

For case 91, both sets of solvers failed. The use of weighting does appear to have aided the magVF solver significantly, however it still does not meet the target threshold for $RMSE_2$, and neither does VF/WVF.

Case 100 consisted of complex and real repeated poles and complex repeated zeros, with a real zero.

Test case #	100
Given Poles	-100+100j, -100-100j, -1E6, -1E6 rad/s
Given Zeros	-8E3, -1E4+1E4j, -1E4-1E4j rad/s
Given DC Gain	1.25E4
Given Delay	0 s

Table 4.6: Complex repeated poles, test case #100

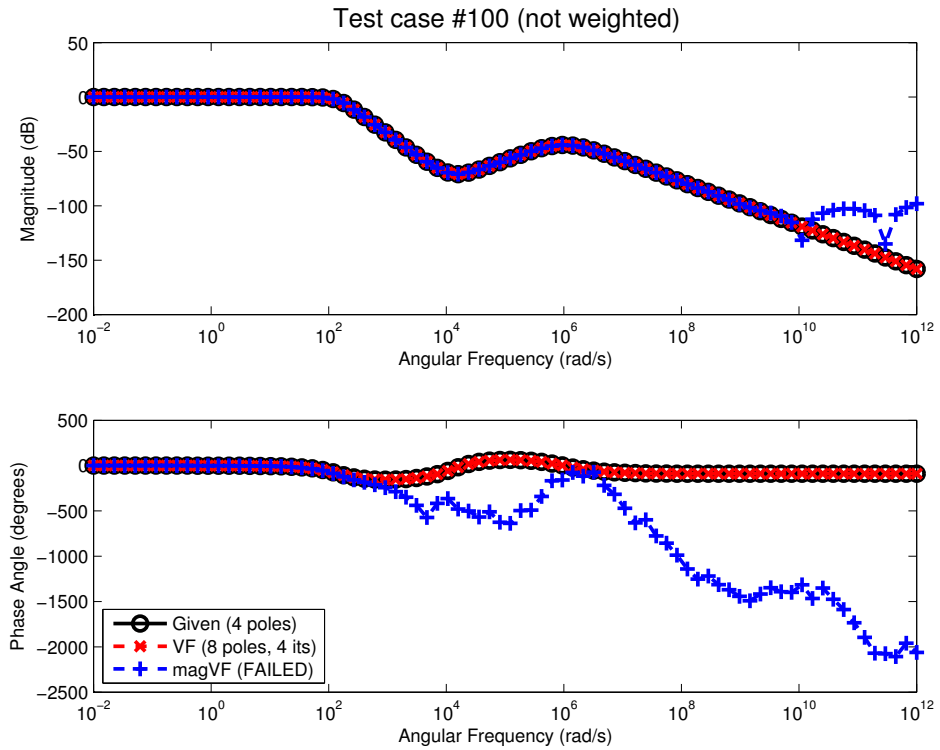

(a) without weighting

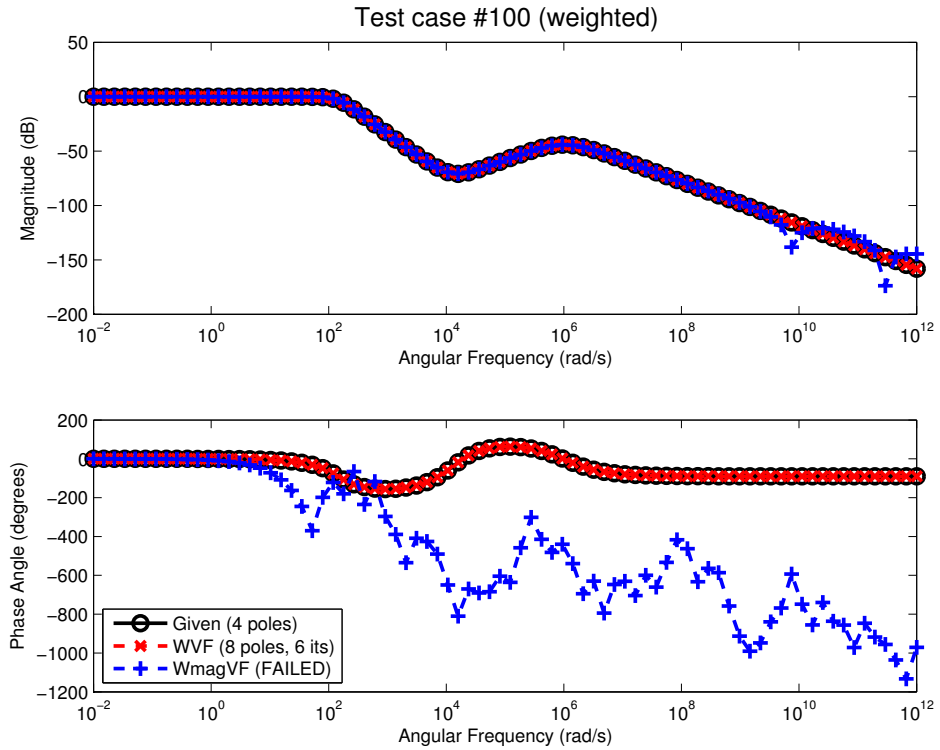

(b) with weighting

Figure 4.7: Repeated poles, with increased order. Actual pole order is 4 (2 repeated real poles and one pair of complex conjugate poles). Notice that VF and WVF require twice as many poles, and magVF and WmagVF fail to converge

Test case #	110
Given Poles	-1E3 -1E3 -1E6 -1E6 rad/s
Given Zeros	-8E3, -1E4, -1E4 rad/s
Given DC Gain	1.25E6
Given Delay	0 s

Table 4.7: Real repeated poles, test case #110

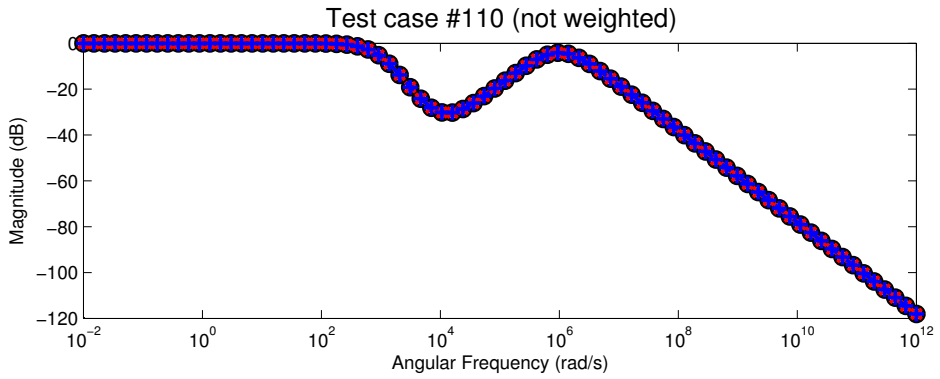

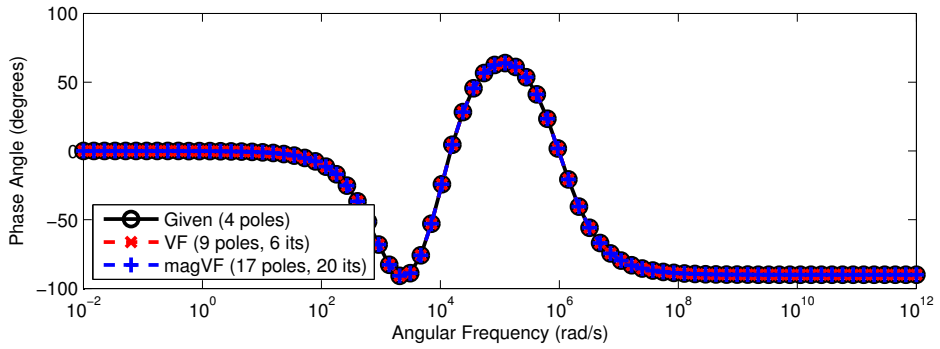

(a) without weighting

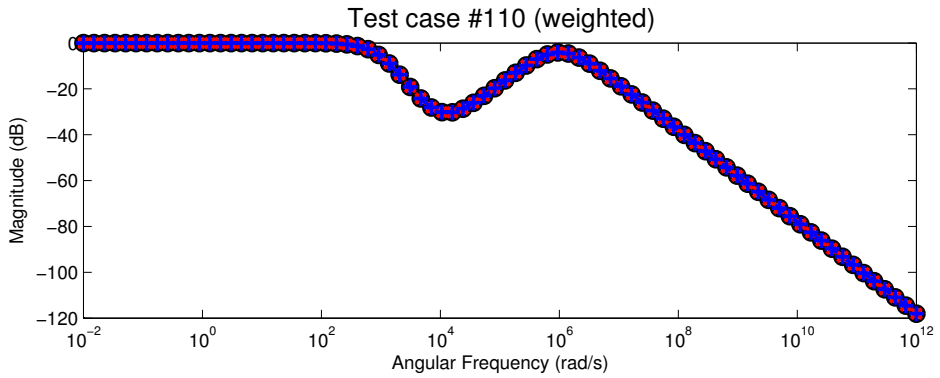

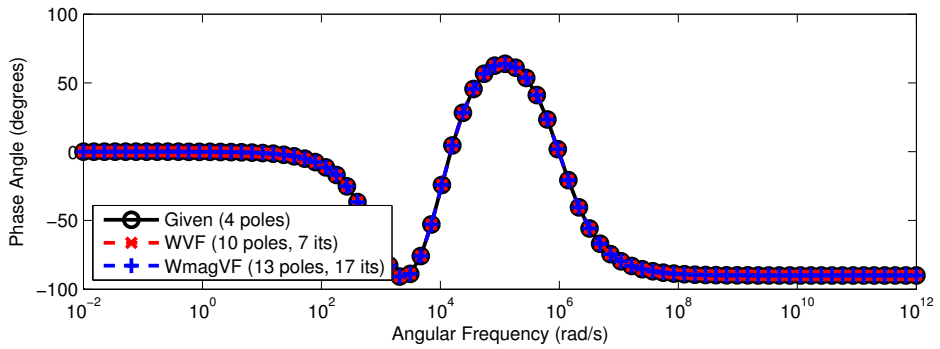

(b) with weighting

Figure 4.8: Repeated poles, with increased order. Actual order is 4 (2 repeated real poles and one pair of complex conjugate poles)

It appears that magVF suffers more considerably from the inclusion of repeated poles than VF. The VF algorithm required twice as many poles as actually existed in the original function, while magVF depended on even more. The inclusion of weighting did appear to improve the performance, such that WmagVF required significantly fewer poles to achieve a good fit. However, this was not always guaranteed, as certain functions did not achieve successful convergence even though they appeared to be improved.

From these results, it can be concluded that both VF and magVF perform poorly when confronted with poles of higher order multiplicity. This can be expected, since as pointed out in [24], the basis functions for VF (and magVF for that matter) are composed of single order poles in a partial fraction form. These basis functions do not consider the higher order s-terms that would normally appear in the numerator when performing the PFE with poles of higher order multiplicity. Accommodating for a modified basis is not trivial, and a reformulation of the magVF basis functions for such cases has not been pursued further in this study other than to increase awareness of the limitations of magVF.

4.4 Discussion

From these tests, it was possible to confirm the following:

- W/magVF cannot resolve mixed-phase systems, including ones which have poles or zeros close to the imaginary axis. This is due to the method by which the poles and zeros are selected when going from the magnitude-squared poles and zeros – which are symmetric about the imaginary axis – to its square-root. Practical limitations of this observation mean that mixed-phase systems, or those with oscillating responses, are not possible to approximate with the current implementation of W/magVF. Note that, a way to be able to resolve a mixed phase system could be implemented that examines the difference in the phase of the approximated and actual systems, and iteratively swaps the appropriate zeros from the magnitude-squared results until best convergence is achieved between the square-root magnitude approximation, and phase approximation, simultaneously. This has not been implemented here, and is left for future study as required.

- W/magVF and W/VF demonstrated difficulties with poles of higher order multiplicity and complexity. This issue has been discussed with respect to Vector Fitting in [24], and perhaps analogous modifications can be ported to the W/magVF basis functions to improve the functionality of this method. Practically, this means that certain types of functions may not be so easy to approximate, such as those where the magnitude or phase is changing rapidly, as would be expected with repeated or complex poles.

- W/magVF offers a simple method for calculating delays. A practical implication of this could be that W/magVF could serve as a replacement for the W/VF root-finding approach to *a priori* delay determination during its fitting procedure.

CHAPTER 5

FITTING OF LINE AND CABLE PROPAGATION FUNCTIONS

5.1 Overview

Ultimately, the purpose of this study is to demonstrate the utility of W/magVF for fitting transmission line and cable propagation functions. Two sets of actual cable data and one transmission line case were submitted to a series of tests using the various algorithms detailed in this thesis (VF, WVF, magVF, and WmagVF, with and without IPM). The goal of the study was to determine if it was possible to approximate propagation functions using these techniques, and under what conditions and limitations they excelled or not. Furthermore, a greater understanding of the mechanics of propagation functions and their approximations was desired.

5.2 Background information about cable and transmission line case data studied

Three different sets of data were used to examine the utility of the fitting algorithms developed. Relevant information regarding the cases CAB01, CAB02, and TRL01 is given in the following figures and tables, and further details can be found in [23].

5.2.1 CAB01

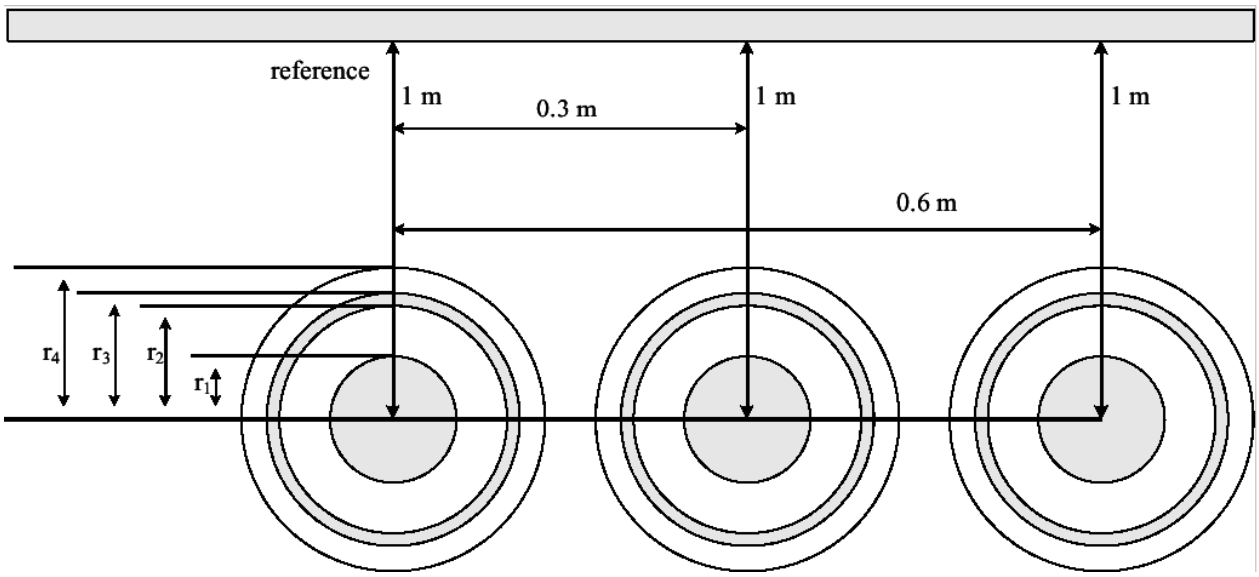

Figure 5.1: Configuration of underground power cables studied, CAB01 case

Table 5.1: CAB01 cable details

Definition	**Value**
Inner Radius of the Core	0 mm
Outer Radius of the Core	19.50 mm
Inner Radius of the Sheath	37.75 mm
Outer Radius of the Sheath	37.97 mm
Outer Insulation Radius	42.50 mm
Resistivity of Core	$1.718E-8\ \Omega \cdot m$
Resistivity of Sheath	$3.365E-8\ \Omega \cdot m$
Relative Permeability	1
Insulator Relative Permeability	1
Core Insulator Relative Permittivity	2.85
Shield Insulator Relative Permittivity	2.51
Insulation Loss Factor	0.001
Cable Length	10 km
Earth Resistivity	$100\ \Omega \cdot m$

5.2.2 CAB02

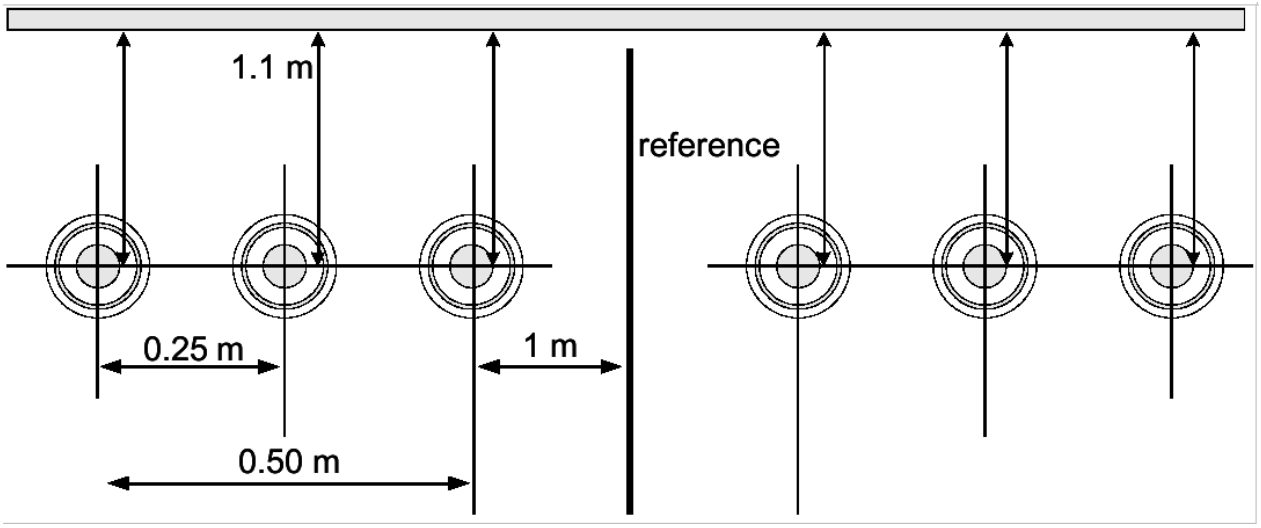

Figure 5.2: Configuration of underground power cables studied, CAB02 case

Table 5.2: CAB02 cable details

Definition	Value
Inner Radius of the Core	3.175 mm
Outer Radius of the Core	12.54 mm
Inner Radius of the Sheath	22.735 mm
Outer Radius of the Sheath	26.225 mm
Outer Insulation Radius	29.335 mm
Resistivity of Core	$1.718E-8\ \Omega \cdot m$
Resistivity of Sheath	$3.365E-8\ \Omega \cdot m$
Relative Permeability	1
Insulator Relative Permeability	1
Core Insulator Relative Permittivity	3.5
Shield Insulator Relative Permittivity	2
Insulation Loss Factor	0.001
Cable Length	15 km
Earth Resistivity	$250\ \Omega \cdot m$

5.2.3 TRL01

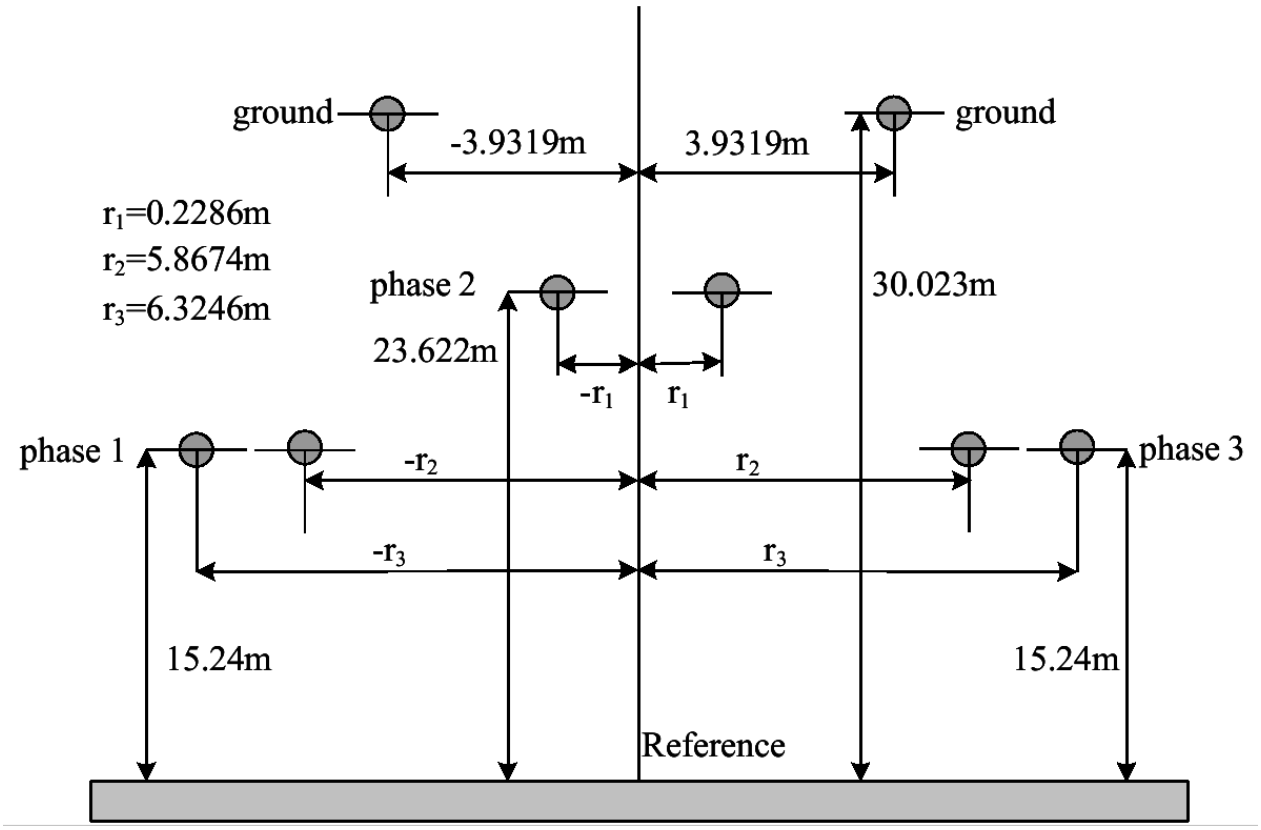

Figure 5.3: Configuration of overhead transmission lines studied, TRL01 case

Table 5.3: TRL01 overhead transmission lines details

Definition	Value
Outside Diameter of the Phase Conductors	4.06908 cm
Outside Diameter of the Ground Conductor	0.98044 cm
DC Resistance Phase	0.0324 Ohm/km
DC Resistance Ground	1.6216 Ohm/km
Model Frequency	60 Hz
Line Length	200 km
Earth Resistivity	100 $\Omega \cdot m$
Skin Effect Correction Factor - Phase	0.363 (Thick/Diam)
Skin Effect Correction Factor - Ground	0.5 (Thick/Diam)

5.3 Different domains of ULM involved in this study

Using the ULM method, as discussed in Section 2.2, fitting of propagation functions is broken down into different domains, namely: the phase domain, the modal domain and the time domain.

As a review, the overall procedure for fitting a set of cables or transmission lines given the frequency domain distributed parameters is as follows.

1. Suppose that distributed frequency-dependent phase-domain shunt admittance matrix, $\mathbf{Y}$, and series impedance matrix, $\mathbf{Z}$, are available for a given transmission line or cable per unit length.

2. Then, given a length, l, these matrices can be converted into the propagation matrix $\mathbf{H}$ and characteristic admittance matrix $\mathbf{Y_c}$, with responses using equations (2.1) and (2.2), which are also in the phase domain, given a range of frequencies that can be very large .

3. The characteristic admittance matrix can be calculated directly using a fitter such as W/VF in the phase domain. However, the propagation matrix is more complicated as it has additional delays that need to be determined in addition to the poles and residues. Using frequency dependent transformation matrices it becomes possible to decompose the propagation matrix $\mathbf{H}$ response into individual SISO modal domain responses. For the propagation matrix, these responses are attributed to different MPFs, the poles and delays of which will be used later for reconstructing the MIMO propagation function $\mathbf{H}$.

4. The modal domain MPFs are fit using W/VF or W/magVF, in order to discover the poles and delays associated with the MPF form of (2.5). Recall that these MPFs are assumed to be MPS functions. Hence, it should be possible to fit them with transfer functions having all poles and zeros in the LHP.

5. The propagation matrix $\mathbf{H}$ can then be fitted using (2.7), by a final overdetermined LLS solution with the poles and time delays having already been determined for each MPF. All that remains is to solve for the unknown residues, in the phase domain.

6. Now it is possible to apply convolutions to derive the current or voltage and either the sending or receiving end of the cable or line, in the time domain using the phase domain matrices for $\mathbf{Y_c}$ and $\mathbf{H}$.

This study focuses on steps 3, 4, and 5. The focus is entirely on the application of W/magVF on the fitting of the modal domain MPFs and their re-assembly into the propagation matrix. In general, lower order approximations, with fewer complex poles, can provide significant gains in the time domain [25].

5.3.1 VF and WVF approach to fitting modal propagation functions

For VF (and WVF), it is essential to select a good estimate for the modal time delay (τ_m) prior to attempting to fit the mode. The delay must be removed from H_m of (2.5), and then the fitter can be run on H'_m. Fig. 5.1 shows an overview of this algorithm.

Algorithm 5.1 Algorithm for fitting H'_m using VF or WVF

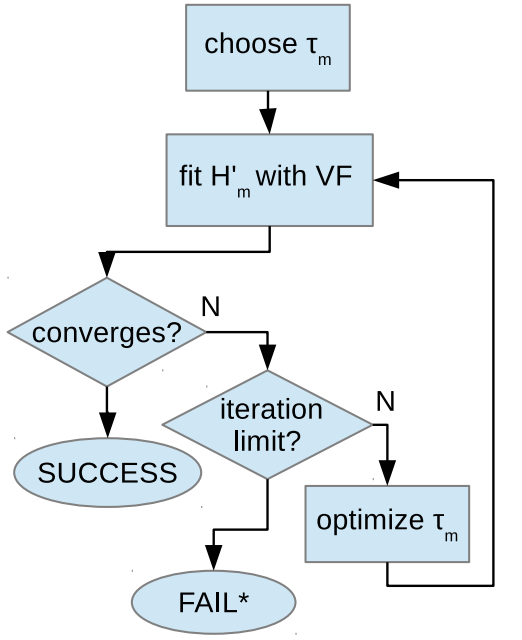

Without an appropriate choice of τ_m, the fit will not be successful, as illustrated by Fig. 5.4.

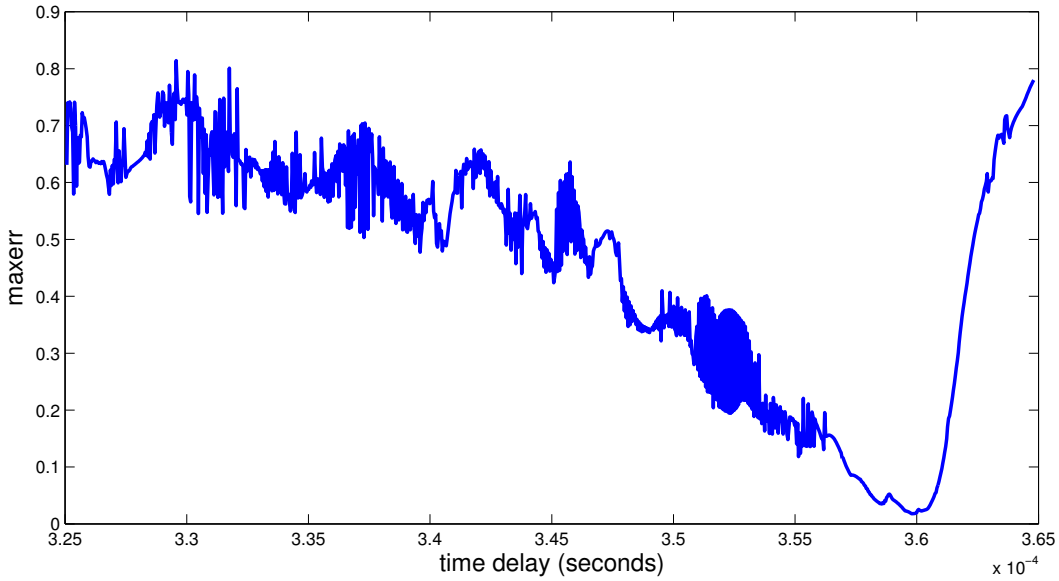

Figure 5.4: Typical example of VF *maxerr* with respect to choice of time delay, τ_m

In EMT-type program applications the time delay is processed in order to minimize the fitting error using Brent's method for root-finding. This involves first estimating the time delay, then applying iterative modification of the time delay in successively smaller intervals, adding the delay to the modal propagation function, performing VF/WVF, and then subtracting the delay before testing for convergence.

5.3.2 Getting the final approximation from a magnitude squared one

The magVF (and WmagVF) approach exploits the assumption that the propagation functions are minimum phase to allow the fitting to proceed without prior time delay estimation. The magVF algorithm yields magnitude-squared poles and zeros which are symmetric with respect to the imaginary axis in the Laplace domain, as per (2.32).

To get the magnitude and phase response of a minimum phase function from the magnitude-squared response after fitting with magVF, two approaches can be taken.

First, to get the the magnitude approximation from the magnitude-squared approximation, one way is to take the square-root at each frequency point, as in

$$\sqrt{|H_m(\omega_k)|^2} = |H_m(\omega_k)|\,. \tag{5.1}$$

Then, using the fact that minimum-phase systems have a direct relationship between their magnitude and phase responses, it is theoretically possible to derive the phase response from this result [26, 27]. This method was not employed in the current study.

The alternative solution is to convert (2.34) into an equivalent poles-zeros-gain form and then select only the LHP poles and zeros. This is equivalent to going from (2.32) to (2.33). The DC gain, F_0 from (2.33), is determined by taking the ratio between the given response and the approximated one at any frequency point where the given response has sufficient magnitude, to reduce numerical errors inherent in calculating with overly large or small numbers. For this study, the magnitude responses were normalized at low frequencies and have the form of low-pass filters, and so these values were employed for recovering F_0.

Once the phase of the minimum phase function H'_m has been determined, and supposing that $\measuredangle H'_m$ refers to the phase of the minimum-phase system that has been derived using magVF, and $\measuredangle H_m$ is the phase of the given modal function, then it is possible to employ the ULM theory from (2.5), such that

$$\measuredangle H_m = \measuredangle H'_m - \omega\tau_m \tag{5.2}$$

$$\tau_m = \frac{\measuredangle H'_m - \measuredangle H_m}{\omega} \tag{5.3}$$

Given that τ_m is practically constant, it can be solved as an overdetermined least squares problem using all or a select number of frequency points. The algorithm for determining the delay in this study was to solve for it at each frequency sample, as well as by splitting the frequency range into quarters and solving for it in each quarter of the frequency range, as an overdetermined systems problem. The resulting value which yielded the lowest error when combined with the W/magVF approximated system was the one which was selected.

5.4 Initial tests in the modal domain with CAB01

Initially, to observe the behaviour of the fitters strictly in the modal domain, two types of tests were conducted using CAB01:

1. The first involves fixing an arbitrary order, and trying to fit each modal propagation function with magVF, using different strategies (DCP optimization, weighting, input pole modifications) to see the effects on convergence.

2. The second test involves a comparison of the various fitters (VF/WVF/magVF/W-magVF, with and without pole modification) to determine the lowest number of poles required to arrive at a successful fit within a defined error limit.

5.4.1 Fitting using magVF with arbitrary order to see effect of incremental modifications

The algorithm used for determining the effect that the various modifications to magVF had on the final results is shown in Fig. 5.2. Table 5.4 gives results for the MAE_1 observed using this procedure.

Algorithm 5.2 Testing algorithm used to determine effect of magVF modifications with fixed order

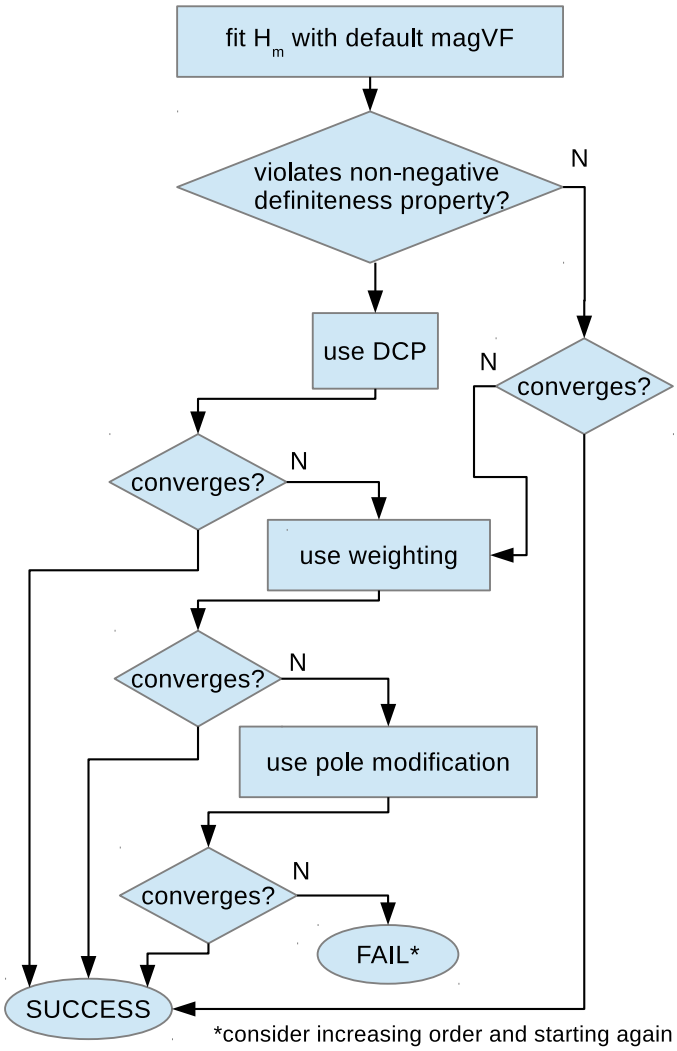

Each MPF was fit with 12 poles, initially all real and distributed logarithmically. An MAE_1 of 0.0250 was defined as the threshold for successful convergence. A maximum of 300 iterations was allowed, but not necessarily required, since convergence was tested after each iteration.

Table 5.4: Resulting MAE between given and fitted modal frequency response using magVF as per algorithm described in Fig. 5.2. Desired $MAE_1 < 0.0250$.

MPF #	**Default** MAE_1	**Needs DCP?**	**DCP** MAE_1	**Weighted** MAE_1	**IPM (type 2)** MAE_1
1	0.0166	**Yes**	0.0016	0.0016	0.0016
2	**0.0272**	**Yes**	**0.0269**	**0.0239**	0.0210
3	**0.0918**	No	**0.0918**	**0.0459**	0.0212
4	0.0052	No	0.0052	0.0052	0.0052
5	0.0052	No	0.0052	0.0052	0.0052
6	0.0052	No	0.0052	0.0052	0.0052

Examining Table 5.4, it can be seen that MPFs 2 and 3 failed to meet the desired target for maximum error using the default configuration. Functions 1 and 2 failed to meet the non-negative definite criteria, and needed the DCP constraints. After applying the constrained fitter, function 1 and 2 achieved improved convergence.

Next, weighting was applied to all modal domain functions. Although function 3 made a significant improvement with the application of weighting, it still remained above the desired threshold of 0.0250. Function 2 was reduced to 0.0239, and thus achieved convergence thanks to the application of WmagVF. Since the other functions which converged had done so after the first iteration, weighting had no effect on them.

Finally, applying the pole modification scheme was required in addition to weighting to fit the remaining two functions. Function 2 converged after three iterations, while function 3 required 175 iterations before converging using this pole modification technique.

The resulting magnitude and phase plots are given in Fig. 5.5.

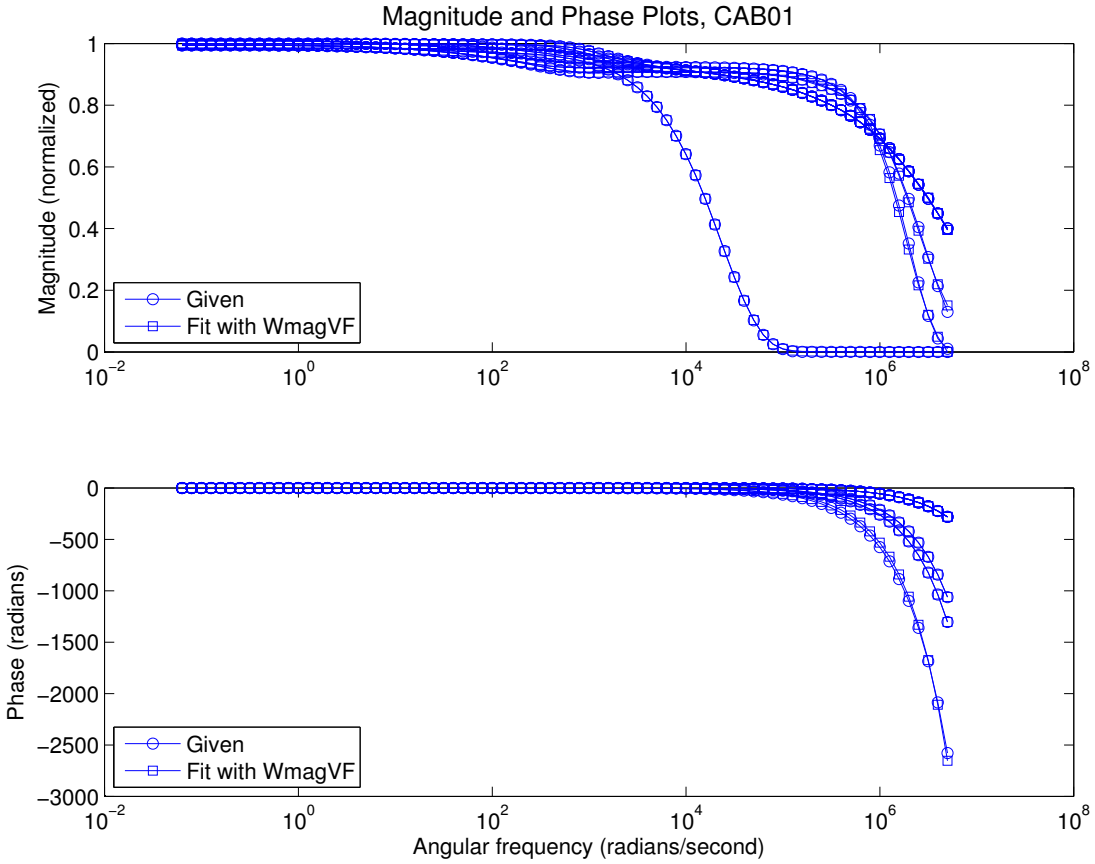

Figure 5.5: Magnitude and phase plots of all 6 modal propagation functions using 12 poles to fit ($Norder = 12$). Given modal data is superimposed with WmagVF approximation (see Table 5.4 for errors)

5.4.2 Minimum order required to achieve convergence using VF/WVF/magVF/W-magVF and pole modification

Another set of tests was run to see how the fitters performed with respect to minimizing the order required to arrive at a solution within a desired error. The algorithm for this is presented in Algorithm (5.3).

Algorithm 5.3 Algorithm for testing minimum order required to converge within desired error

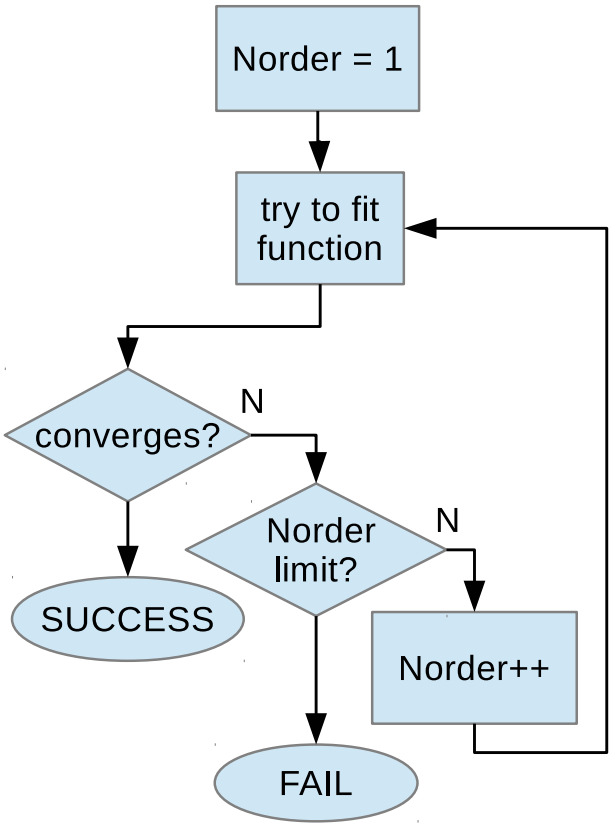

The limit for the approximation order was defined as one-half of the total number of frequency samples available ($K = 80$), such that

$$Norder_{max} < \frac{K}{2} = 40 \text{ poles.} \tag{5.4}$$

The results are summarized in Fig. 5.6a for VF and WVF, and Fig. 5.6b for magVF and WmagVF. It can be seen that in all but one case (WVF with pole modification, mode 2), the fitters were successful in finding solutions that converged within the desired maximum error limits ($MAE_1 < 0.025$). Furthermore, the number of poles required by weighted fitting was consistently less than by non-weighted fitting.

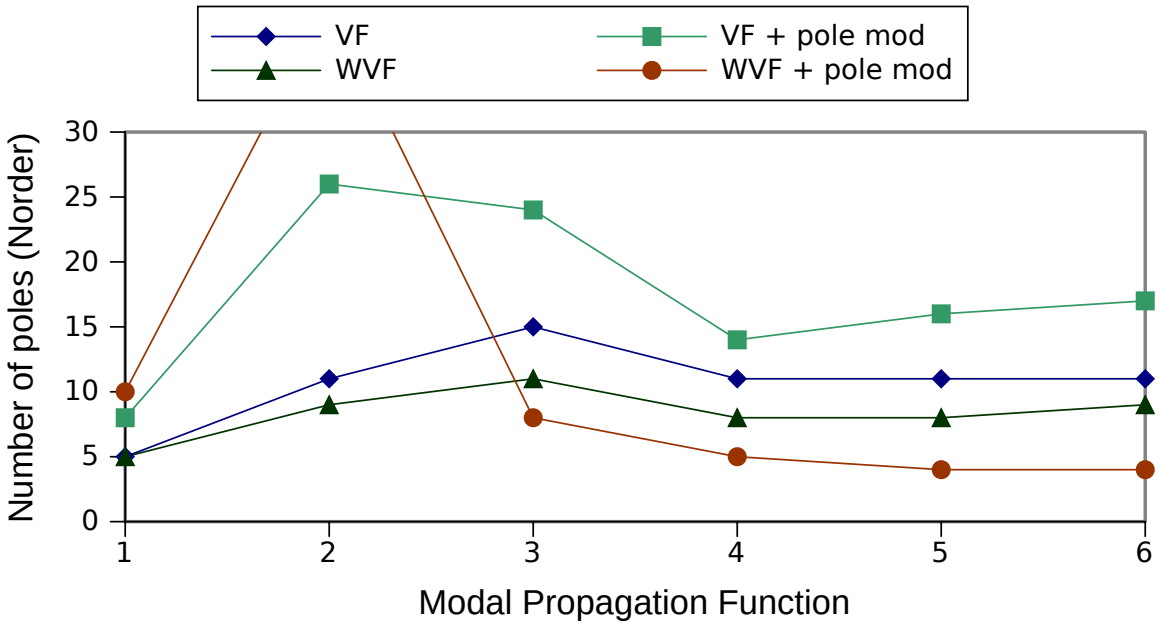

(a) Using VF/WVF. Note that the second modal propagation function does not have a solution for WVF with pole modification. It does not appear on this figure as a result, since it never converged within the defined constraints ($Norder < \frac{K}{2}$)

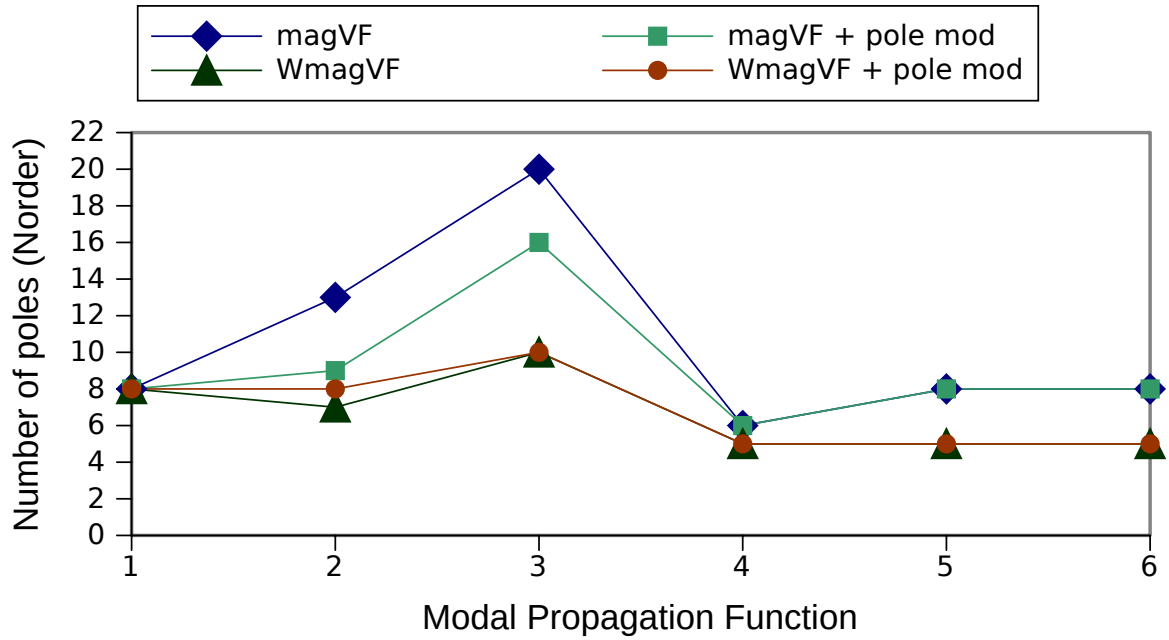

(b) Using magVF/WmagVF, with/without pole modification.

Figure 5.6: Minimum order required for convergence with $MAE_1 < 0.025$. Lower values are better.

5.4.3 Discussion of results

5.4.3.1 Benefits of using weighting

It is evident that weighting showed an improvement with both VF and magVF. This is especially true for troublesome functions – numbers 2 and 3 in this case study. From both tests conducted, and with both families of fitters, weighting was able to demonstrate improved performance.

5.4.3.2 Benefits of using pole modification for smooth response

A pole modification scheme of fitting based on smooth responses using real input poles was demonstrated in this thesis. It proved to be beneficial in nearly all cases. It was required for modal function 3 when the order was fixed at 12 poles.

However, when employed with WVF there was one case (function 2) where this modification did not manage to provide a suitable solution. When, and how, this pole modification scheme is employed – which is effectively a perturbation of the fitter between iterations – should be examined in further detail to develop best practises accounting for the internal mechanics of the fitter and type of responses being fit.

5.4.3.3 W/VF does not guarantee minimum-phase systems

Taking the zeros of the approximated transfer functions provided by the VF or WVF algorithms it was observed that for many of the cases there were zeros in the right-hand s-plane. This implies that the modal approximations being returned by VF or WVF were often non-minimum phase, or mixed phase systems. The magVF and WmagVF algorithms, on the other hand, guarantee minimum-phase systems with zeros that are strictly in the LHP. More research is needed to see the effect of pole-zero cancellation, and to study the implications of using mixed-phase approximations with the ULM.

5.4.3.4 W/magVF converges quickly for certain modal propagation functions

It was observed that during the second set of tests, as presented in Section 5.4.2, the W/magVF algorithm converged very quickly, often in the first iteration. As mentioned previously, this implies that weighting is often unnecessary, since it has no effect until the second iteration. Furthermore, it suggests that W/magVF may be much quicker than the current VF/WVF method which requires an iterative approach to find a suitable value for time delay τ_m. Although, with magVF, certain modal propagation functions may require

optimization of the residues to ensure non-negative definite values, this procedure is not more stringent than the iterative estimation of the time delays used in VF.

5.5 Thorough tests in the phase domain

The three cases (CAB01, CAB02, and TRL01) were fit using different configuration parameters. A four digit code was developed to distinguish the results accordingly. Table 5.5 gives the meaning of each digit, and its possible states.

Table 5.5: Significance of 4 digit testing codes

Digit's location in code	Most Significant	.....		Least Significant
Type	Bit	Bit	Bit	Trit
Meaning	Auto DCP optimization?	Phase included in error during convergence tests?	Weighting method?	Input Pole Modification ?
Possible States	0=No, 1=Yes	0=No, 1=Yes	0=No, 1=Yes	0=No, 1= Yes, strip imaginary parts out, 2=Yes, take negative of the magnitudes

The code as given in Table 5.5 is comprised of 4 mutually exclusive variable states. The three most significant digits are binary values (0 or 1), and the least significant (ie., rightmost) is a ternary value (0,1, or 2). In addition, a special code is also used: FS implies a Final Sweep, which was composed of a heterogeneous mix of MPF configurations, based on selecting the ones that yielded the lowest MAE_2 for each MPF, given all possible configuration results and then performing a final phase domain fit. Note that for W/VF fitting, the most significant configuration digit is irrelevant, and so that family of fitters has only a three-digit code, while the W/magVF family uses all four digits.

The following results are organized by case (CAB01, CAB02, TRL01). For each case, the results from each family of fitter (W/magVF, W/VF) are given concurrently. Two sets of graphs are shown. The first graph set gives the configurations sorted by lowest overall MAE_2

(in the phase domain, after fitting the propagation matrix). The second set of graphs gives a comparison of the average number of effective poles ($N_{order,eff}$, after pole-zero cancellations are taken into account) and the average number of complex poles ($N_{complex,eff}$), where a complex pole is defined such that its imaginary part is significant enough to be considered as such. This way, numerical error in the precision of the numbers in the complex plane was controlled for. Subsequently, the best and worst homogeneous configurations, with respect to MAE_2 results in phase domain, are presented with tables to show the details of the actual fitting for each MPF. In addition, a table is provided giving the FS hybrid configuration results for each case and fitter type.

5.5.1 Phase-domain fitting results

The following sections provide the phase-domain fitting results for each case studied. Results are given for W/VF first, followed by W/magVF.

5.5.1.1 CAB01

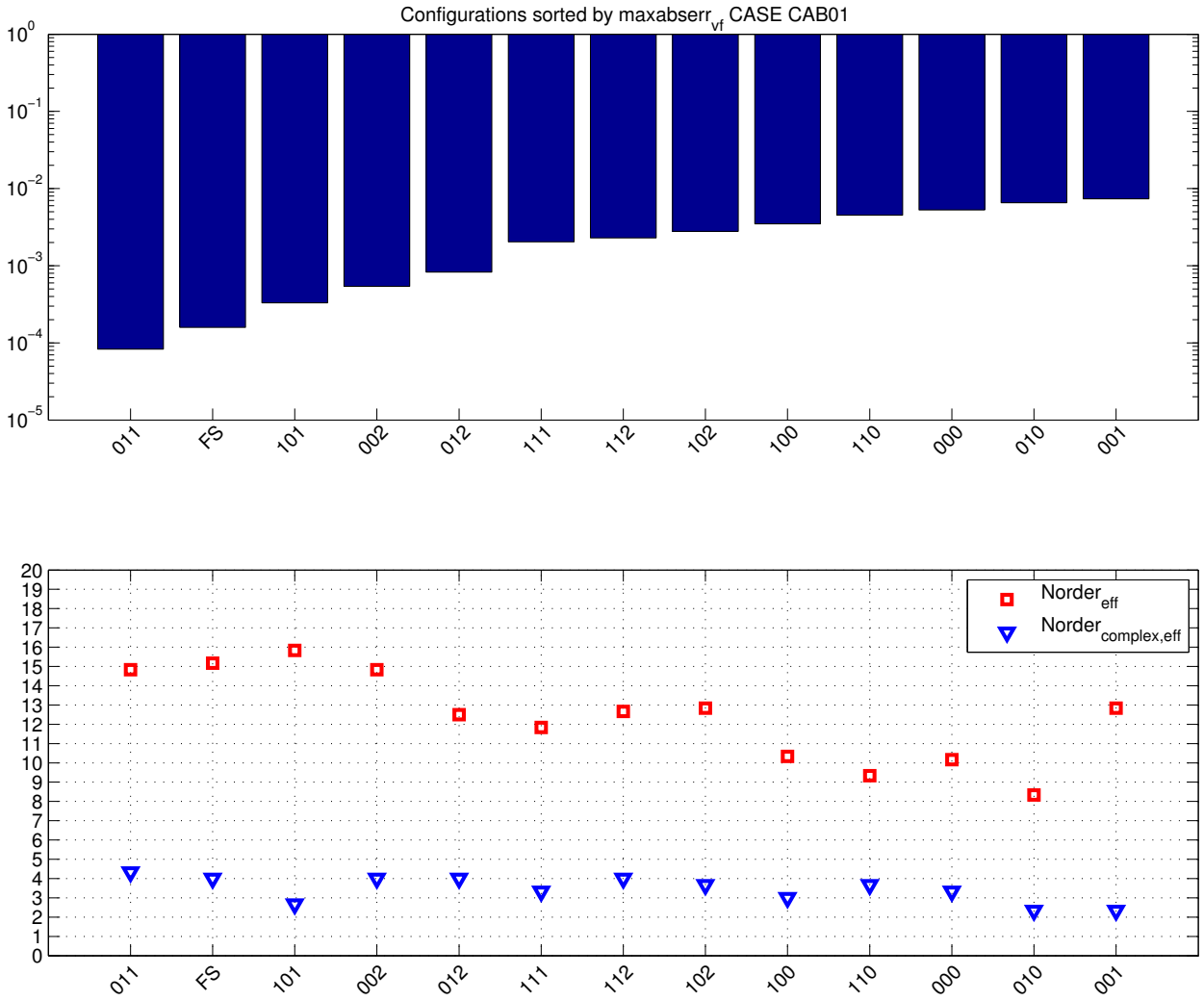

Figure 5.7: W/VF maxabserr results in the phase domain, all configurations, CAB01

Table 5.6: Select configurations, W/VF, CAB01

(a) 011 (phase-domain best case)

MPF	N_{order}	$N_{order,eff}$	τ_m [s]	$N_{complex,eff}$	Relative Order	$Cancellations_{PZ}$	MAE_1	MAE_2	RHP Zeros
1	11	11	$5.925 \cdot 10^{-4}$	2	1	0	$4.863 \cdot 10^{-3}$	$4.863 \cdot 10^{-3}$	2
2	20	19	$2.594 \cdot 10^{-4}$	6	1	1	$9.195 \cdot 10^{-3}$	$9.988 \cdot 10^{-3}$	4
3	20	20	$2.061 \cdot 10^{-4}$	6	1	0	$3.430 \cdot 10^{-1}$	$4.721 \cdot 10^{-1}$	5
4	11	10	$5.571 \cdot 10^{-5}$	2	1	1	$3.786 \cdot 10^{-3}$	$4.060 \cdot 10^{-3}$	2
5	10	10	$5.568 \cdot 10^{-5}$	2	1	0	$4.595 \cdot 10^{-3}$	$5.228 \cdot 10^{-3}$	2
6	20	19	$4.890 \cdot 10^{-5}$	8	1	1	$4.713 \cdot 10^{-1}$	$6.553 \cdot 10^{-1}$	4
Mean	15.33	14.83	$2.030 \cdot 10^{-4}$	4.33	1	0.5	$1.395 \cdot 10^{-1}$	$1.919 \cdot 10^{-1}$	3.17

(b) FS

MPF	N_{order}	$N_{order,eff}$	τ_m [s]	$N_{complex,eff}$	Relative Order	$Cancellations_{PZ}$	MAE_1	MAE_2	RHP Zeros	CONFIG
1	10	10	$6.005 \cdot 10^{-4}$	2	1	0	$2.873 \cdot 10^{-3}$	$3.358 \cdot 10^{-3}$	2	012
2	20	19	$2.594 \cdot 10^{-4}$	6	1	1	$9.196 \cdot 10^{-3}$	$9.501 \cdot 10^{-3}$	4	002
3	20	19	$2.108 \cdot 10^{-4}$	6	1	1	$7.296 \cdot 10^{-3}$	$7.296 \cdot 10^{-3}$	4	112
4	14	13	$5.571 \cdot 10^{-5}$	2	1	1	$3.053 \cdot 10^{-3}$	$3.597 \cdot 10^{-3}$	2	002
5	16	15	$5.571 \cdot 10^{-5}$	4	1	1	$2.818 \cdot 10^{-3}$	$3.411 \cdot 10^{-3}$	2	002
6	17	15	$5.572 \cdot 10^{-5}$	4	1	2	$2.848 \cdot 10^{-3}$	$3.426 \cdot 10^{-3}$	2	002
Mean	16.17	15.17	$2.063 \cdot 10^{-4}$	4	1	1	$4.681 \cdot 10^{-3}$	$5.098 \cdot 10^{-3}$	2.67	

(c) 001 (phase-domain worst case)

MPF	N_{order}	$N_{order,eff}$	τ_m [s]	$N_{complex,eff}$	Relative Order	$Cancellations_{PZ}$	MAE_1	MAE_2	RHP Zeros
1	8	7	$6.027 \cdot 10^{-4}$	2	1	1	$3.421 \cdot 10^{-3}$	$4.371 \cdot 10^{-3}$	2
2	20	19	$2.595 \cdot 10^{-4}$	6	1	1	$1.644 \cdot 10^{-2}$	$2.875 \cdot 10^{-2}$	3
3	20	20	$2.116 \cdot 10^{-4}$	4	1	0	$1.294 \cdot 10^{-2}$	$2.598 \cdot 10^{-2}$	2
4	11	10	$5.627 \cdot 10^{-5}$	0	1	1	$1.239 \cdot 10^{-2}$	$1.273 \cdot 10^{-2}$	0
5	11	10	$5.627 \cdot 10^{-5}$	0	1	1	$1.246 \cdot 10^{-2}$	$1.280 \cdot 10^{-2}$	0
6	12	11	$5.627 \cdot 10^{-5}$	2	1	1	$1.249 \cdot 10^{-2}$	$1.283 \cdot 10^{-2}$	0
Mean	13.67	12.83	$2.071 \cdot 10^{-4}$	2.33	1	0.83	$1.169 \cdot 10^{-2}$	$1.625 \cdot 10^{-2}$	1.17

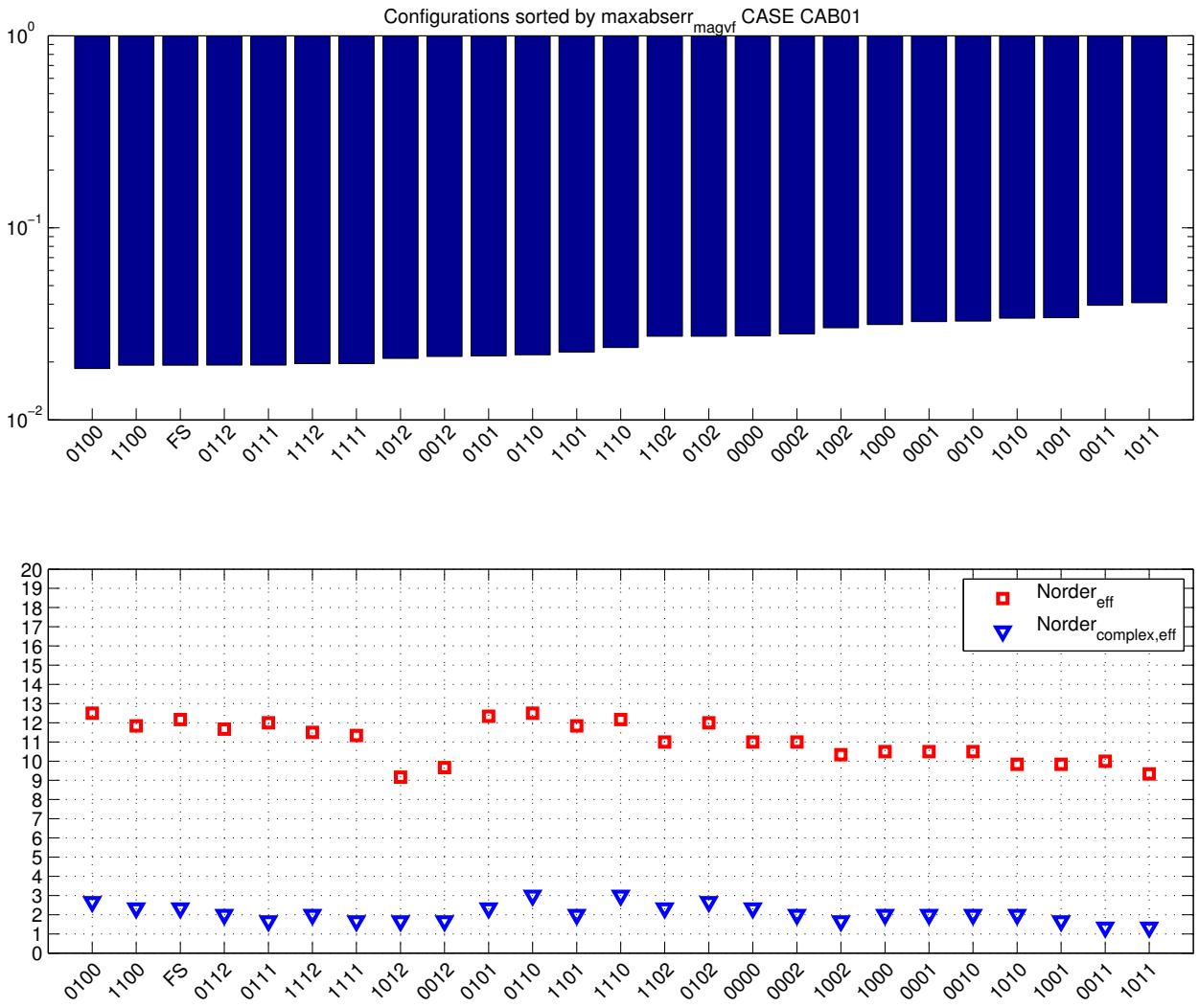

Figure 5.8: W/magVF MAE_2 results in the phase domain, all configurations, CAB01

Table 5.7: Select configurations, W/magVF, CAB01

(a) 0100 (phase-domain best case)

MPF	N_{order}	$N_{order,eff}$	τ_m [s]	$N_{complex,eff}$	Relative Order	$Cancellations_{PZ}$	MAE_1	MAE_2
1	14	11	$6.057 \cdot 10^{-4}$	4	1	3	$3.482 \cdot 10^{-3}$	$3.482 \cdot 10^{-3}$
2	19	17	$2.604 \cdot 10^{-4}$	4	1	2	$5.342 \cdot 10^{-2}$	$5.342 \cdot 10^{-2}$
3	20	19	$2.121 \cdot 10^{-4}$	4	0	1	$5.090 \cdot 10^{-2}$	$5.090 \cdot 10^{-2}$
4	15	10	$5.628 \cdot 10^{-5}$	0	1	5	$1.451 \cdot 10^{-2}$	$1.451 \cdot 10^{-2}$
5	10	10	$5.627 \cdot 10^{-5}$	2	1	0	$1.446 \cdot 10^{-2}$	$1.446 \cdot 10^{-2}$
6	10	8	$5.627 \cdot 10^{-5}$	2	1	2	$1.444 \cdot 10^{-2}$	$1.444 \cdot 10^{-2}$
Mean	14.67	12.5	$2.079 \cdot 10^{-4}$	2.67	0.83	2.17	$2.520 \cdot 10^{-2}$	$2.520 \cdot 10^{-2}$

(b) FS

MPF	N_{order}	$N_{order,eff}$	τ_m [s]	$N_{complex,eff}$	Relative Order	$Cancellations_{PZ}$	MAE_1	MAE_2	CONFIG
1	14	11	$6.057 \cdot 10^{-4}$	4	1	3	$1.054 \cdot 10^{-3}$	$3.482 \cdot 10^{-3}$	0000
2	20	17	$2.604 \cdot 10^{-4}$	4	1	3	$5.002 \cdot 10^{-2}$	$5.002 \cdot 10^{-2}$	0110
3	20	19	$2.121 \cdot 10^{-4}$	4	0	1	$5.090 \cdot 10^{-2}$	$5.090 \cdot 10^{-2}$	0100
4	10	9	$5.627 \cdot 10^{-5}$	0	1	1	$1.440 \cdot 10^{-2}$	$1.440 \cdot 10^{-2}$	0110
5	10	9	$5.627 \cdot 10^{-5}$	2	1	1	$1.428 \cdot 10^{-2}$	$1.428 \cdot 10^{-2}$	0112
6	10	8	$5.627 \cdot 10^{-5}$	0	1	2	$1.428 \cdot 10^{-2}$	$1.428 \cdot 10^{-2}$	0111
Mean	14	12.17	$2.078 \cdot 10^{-4}$	2.33	0.83	1.83	$2.416 \cdot 10^{-2}$	$2.456 \cdot 10^{-2}$	

(c) 1011 (phase-domain worst case)

MPF	N_{order}	$N_{order,eff}$	τ_m [s]	$N_{complex,eff}$	Relative Order	$Cancellations_{PZ}$	MAE_1	MAE_2
1	8	7	$6.047 \cdot 10^{-4}$	2	1	1	$4.509 \cdot 10^{-3}$	$8.097 \cdot 10^{-3}$
2	15	14	$2.605 \cdot 10^{-4}$	4	1	1	$7.987 \cdot 10^{-4}$	$5.768 \cdot 10^{-2}$
3	15	15	$2.122 \cdot 10^{-4}$	2	0	0	$1.536 \cdot 10^{-2}$	$6.421 \cdot 10^{-2}$
4	7	7	$5.628 \cdot 10^{-5}$	0	1	0	$4.389 \cdot 10^{-3}$	$1.495 \cdot 10^{-2}$
5	8	7	$5.627 \cdot 10^{-5}$	0	1	1	$5.619 \cdot 10^{-3}$	$1.465 \cdot 10^{-2}$
6	6	6	$5.628 \cdot 10^{-5}$	0	1	0	$4.607 \cdot 10^{-3}$	$1.525 \cdot 10^{-2}$
Mean	9.83	9.33	$2.077 \cdot 10^{-4}$	1.33	0.83	0.5	$5.881 \cdot 10^{-3}$	$2.914 \cdot 10^{-2}$

5.5.1.2 CAB02

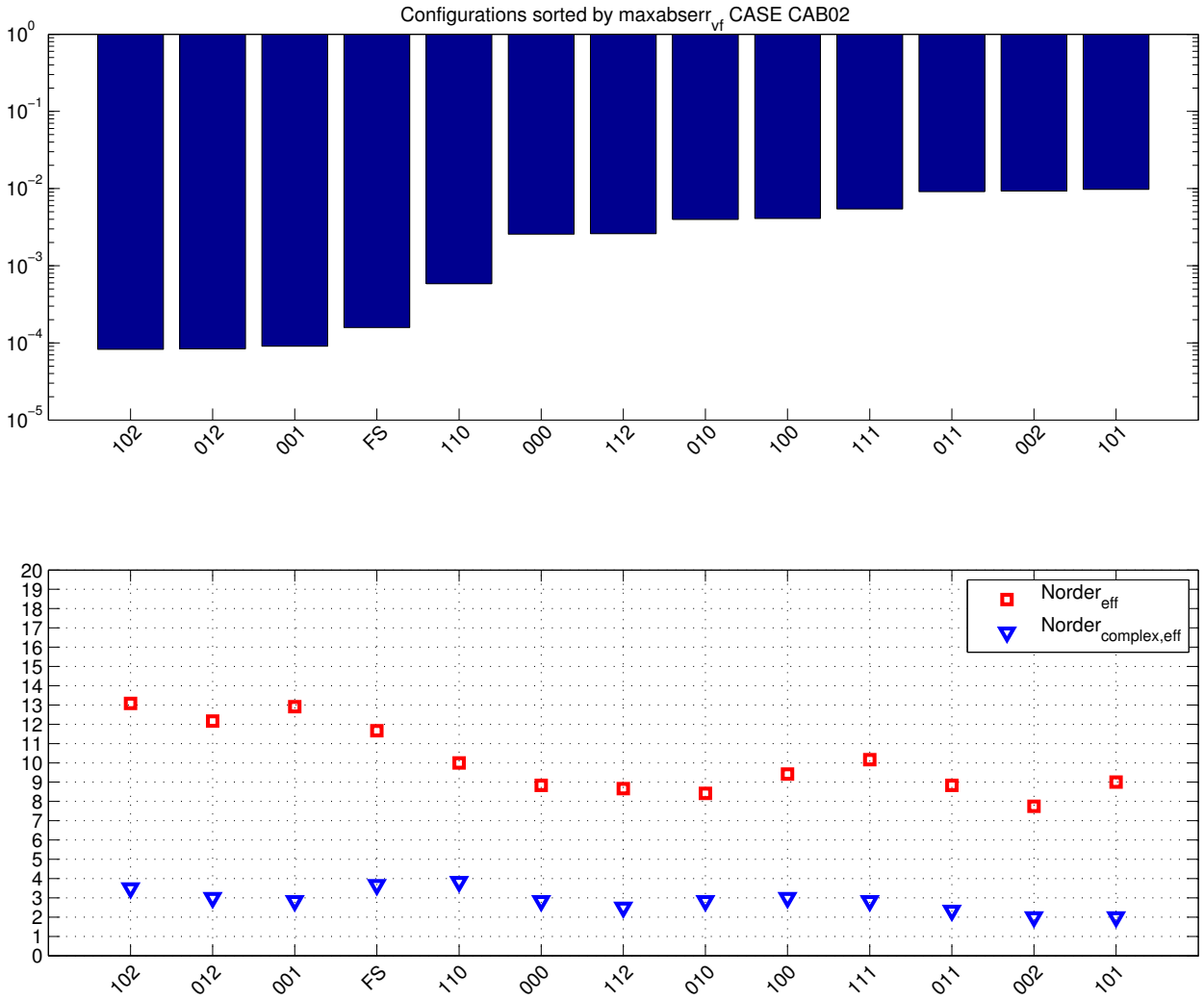

Figure 5.9: W/VF maxabserr results in the phase domain, all configurations, CAB02

Table 5.8: Select configurations, W/VF, CAB02

(a) 102 (phase-domain best case)

MPF	N_{order}	$N_{order,eff}$	τ_m [s]	$N_{complex,eff}$	Relative Order	$Cancellations_{PZ}$	MAE_1	MAE_2	RHP Zeros
1	6	6	$1.096 \cdot 10^{-3}$	2	1	0	$9.475 \cdot 10^{-3}$	$9.475 \cdot 10^{-3}$	2
2	16	16	$6.167 \cdot 10^{-4}$	6	1	0	$1.213 \cdot 10^{-2}$	$1.213 \cdot 10^{-2}$	2
3	20	19	$3.623 \cdot 10^{-4}$	6	1	1	$1.481 \cdot 10^{-2}$	$1.481 \cdot 10^{-2}$	2
4	20	19	$3.594 \cdot 10^{-4}$	6	1	1	$1.540 \cdot 10^{-2}$	$1.540 \cdot 10^{-2}$	2
5	20	20	$2.984 \cdot 10^{-4}$	6	1	0	$1.493 \cdot 10^{-2}$	$1.493 \cdot 10^{-2}$	2
6	20	20	$2.989 \cdot 10^{-4}$	6	1	0	$1.265 \cdot 10^{-2}$	$1.265 \cdot 10^{-2}$	2
7	8	8	$9.375 \cdot 10^{-5}$	0	1	0	$8.307 \cdot 10^{-3}$	$8.307 \cdot 10^{-3}$	0
8	10	9	$9.374 \cdot 10^{-5}$	2	1	1	$8.216 \cdot 10^{-3}$	$8.216 \cdot 10^{-3}$	0
9	11	10	$9.328 \cdot 10^{-5}$	4	1	1	$8.698 \cdot 10^{-3}$	$8.698 \cdot 10^{-3}$	2
10	10	10	$9.375 \cdot 10^{-5}$	0	1	0	$6.941 \cdot 10^{-3}$	$6.941 \cdot 10^{-3}$	0
11	10	10	$9.374 \cdot 10^{-5}$	2	1	0	$8.153 \cdot 10^{-3}$	$8.153 \cdot 10^{-3}$	0
12	10	10	$9.374 \cdot 10^{-5}$	2	1	0	$8.153 \cdot 10^{-3}$	$8.153 \cdot 10^{-3}$	0
Mean	13.42	13.08	$2.995 \cdot 10^{-4}$	3.5	1	0.33	$1.066 \cdot 10^{-2}$	$1.066 \cdot 10^{-2}$	1.17

(b) FS

MPF	N_{order}	$N_{order,eff}$	τ_m [s]	$N_{complex,eff}$	Relative Order	$Cancellations_{PZ}$	MAE_1	MAE_2	RHP Zeros	CONFIG
1	8	7	$1.107 \cdot 10^{-3}$	2	1	1	$2.647 \cdot 10^{-3}$	$3.644 \cdot 10^{-3}$	2	001
2	20	20	$6.170 \cdot 10^{-4}$	8	1	0	$7.926 \cdot 10^{-3}$	$8.025 \cdot 10^{-3}$	2	012
3	13	13	$3.617 \cdot 10^{-4}$	6	1	0	$1.131 \cdot 10^{-2}$	$1.131 \cdot 10^{-2}$	4	110
4	16	16	$3.584 \cdot 10^{-4}$	8	1	0	$1.007 \cdot 10^{-2}$	$1.007 \cdot 10^{-2}$	6	110
5	15	14	$2.982 \cdot 10^{-4}$	6	1	1	$1.247 \cdot 10^{-2}$	$1.247 \cdot 10^{-2}$	4	100
6	14	14	$2.988 \cdot 10^{-4}$	6	1	0	$1.070 \cdot 10^{-2}$	$1.070 \cdot 10^{-2}$	4	100
7	8	8	$9.373 \cdot 10^{-5}$	0	1	0	$7.528 \cdot 10^{-3}$	$8.212 \cdot 10^{-3}$	1	001
8	10	9	$9.374 \cdot 10^{-5}$	2	1	1	$8.216 \cdot 10^{-3}$	$8.216 \cdot 10^{-3}$	0	102
9	9	9	$9.374 \cdot 10^{-5}$	2	1	0	$8.156 \cdot 10^{-3}$	$8.156 \cdot 10^{-3}$	0	100
10	10	10	$9.375 \cdot 10^{-5}$	0	1	0	$6.941 \cdot 10^{-3}$	$6.941 \cdot 10^{-3}$	0	102
11	10	10	$9.374 \cdot 10^{-5}$	2	1	0	$8.153 \cdot 10^{-3}$	$8.153 \cdot 10^{-3}$	0	102
12	10	10	$9.374 \cdot 10^{-5}$	2	1	0	$8.153 \cdot 10^{-3}$	$8.153 \cdot 10^{-3}$	0	102
Mean	11.92	11.67	$3.003 \cdot 10^{-4}$	3.67	1	0.25	$8.523 \cdot 10^{-3}$	$8.671 \cdot 10^{-3}$	1.92	

(c) 101 (phase-domain worst case)

MPF	N_{order}	$N_{order,eff}$	τ_m [s]	$N_{complex,eff}$	Relative Order	$Cancellations_{PZ}$	MAE_1	MAE_2	RHP Zeros
1	6	6	$1.124 \cdot 10^{-3}$	2	1	0	$2.344 \cdot 10^{-2}$	$2.344 \cdot 10^{-2}$	1
2	19	19	$6.180 \cdot 10^{-4}$	6	1	0	$1.579 \cdot 10^{-2}$	$1.579 \cdot 10^{-2}$	2
3	17	17	$3.630 \cdot 10^{-4}$	4	1	0	$2.440 \cdot 10^{-2}$	$2.440 \cdot 10^{-2}$	2
4	17	17	$3.601 \cdot 10^{-4}$	4	1	0	$2.435 \cdot 10^{-2}$	$2.435 \cdot 10^{-2}$	2
5	16	16	$2.989 \cdot 10^{-4}$	4	1	0	$2.051 \cdot 10^{-2}$	$2.051 \cdot 10^{-2}$	2
6	13	13	$2.994 \cdot 10^{-4}$	4	1	0	$2.478 \cdot 10^{-2}$	$2.478 \cdot 10^{-2}$	2
7	4	4	$9.396 \cdot 10^{-5}$	0	1	0	$1.915 \cdot 10^{-2}$	$1.915 \cdot 10^{-2}$	0
8	4	4	$9.395 \cdot 10^{-5}$	0	1	0	$1.998 \cdot 10^{-2}$	$1.998 \cdot 10^{-2}$	0
9	3	3	$9.394 \cdot 10^{-5}$	0	1	0	$1.912 \cdot 10^{-2}$	$1.912 \cdot 10^{-2}$	0
10	3	3	$9.394 \cdot 10^{-5}$	0	1	0	$1.914 \cdot 10^{-2}$	$1.914 \cdot 10^{-2}$	0
11	3	3	$9.396 \cdot 10^{-5}$	0	1	0	$1.949 \cdot 10^{-2}$	$1.949 \cdot 10^{-2}$	0
12	3	3	$9.396 \cdot 10^{-5}$	0	1	0	$1.948 \cdot 10^{-2}$	$1.948 \cdot 10^{-2}$	0
Mean	9	9	$3.023 \cdot 10^{-4}$	2	1	0	$2.080 \cdot 10^{-2}$	$2.080 \cdot 10^{-2}$	0.92

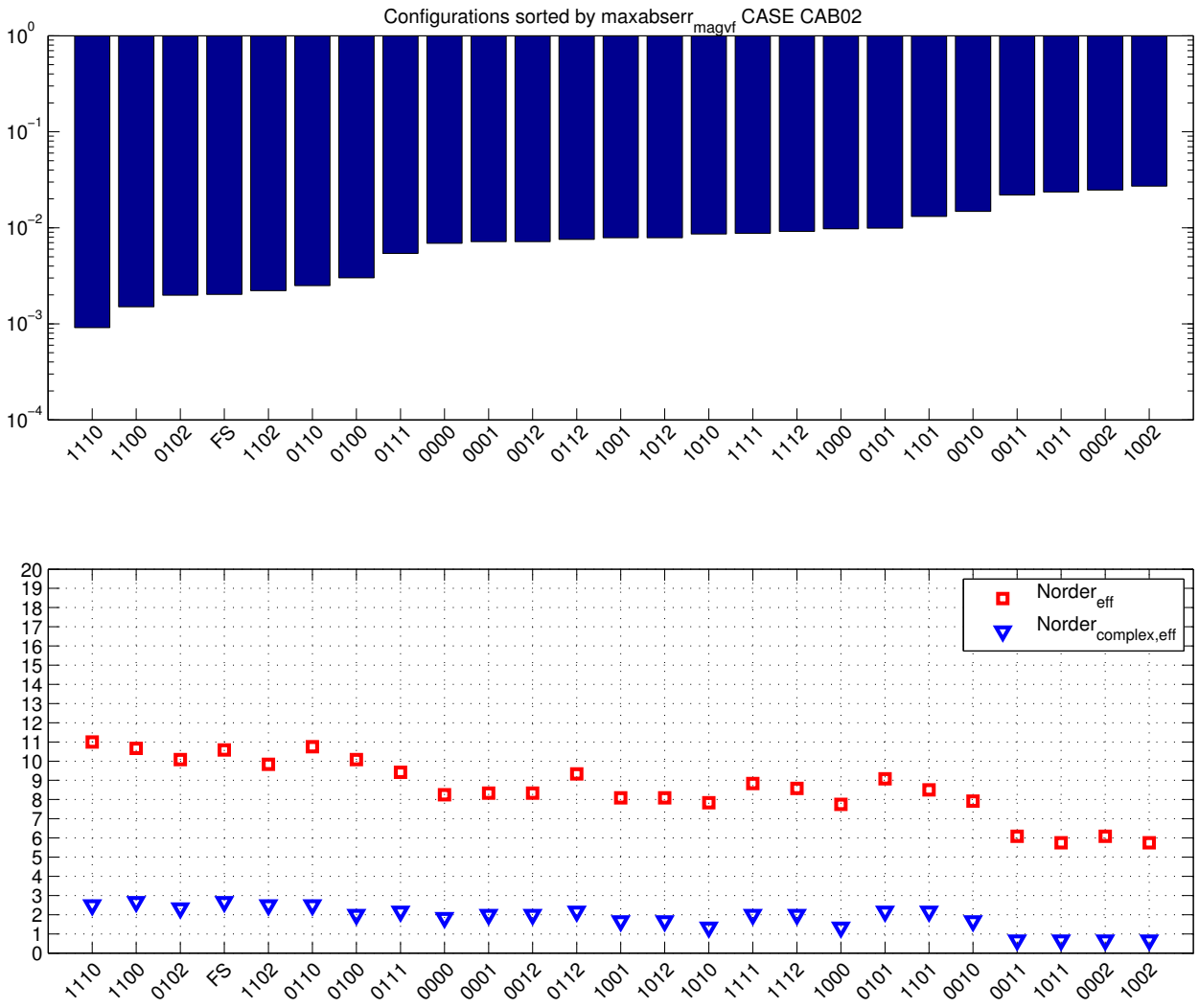

Figure 5.10: W/magVF maxabserr results in the phase domain, all configurations, CAB02

Table 5.9: Select configurations, W/magVF, CAB02

(a) 1110 (phase-domain best case)

MPF	N_{order}	$N_{order,eff}$	τ_m [s]	$N_{complex,eff}$	Relative Order	$Cancellations_{PZ}$	MAE_1	MAE_2
1	7	7	$1.106 \cdot 10^{-3}$	2	1	0	$1.019 \cdot 10^{-2}$	$1.019 \cdot 10^{-2}$
2	20	18	$6.194 \cdot 10^{-4}$	8	1	2	$3.701 \cdot 10^{-2}$	$3.701 \cdot 10^{-2}$
3	18	18	$3.634 \cdot 10^{-4}$	4	1	0	$3.343 \cdot 10^{-2}$	$3.343 \cdot 10^{-2}$
4	15	15	$3.603 \cdot 10^{-4}$	6	1	0	$3.289 \cdot 10^{-2}$	$3.289 \cdot 10^{-2}$
5	18	18	$2.992 \cdot 10^{-4}$	6	1	0	$3.145 \cdot 10^{-2}$	$3.145 \cdot 10^{-2}$
6	15	15	$2.998 \cdot 10^{-4}$	4	1	0	$2.498 \cdot 10^{-2}$	$2.498 \cdot 10^{-2}$
7	7	6	$9.371 \cdot 10^{-5}$	0	2	1	$1.132 \cdot 10^{-2}$	$1.132 \cdot 10^{-2}$
8	7	6	$9.371 \cdot 10^{-5}$	0	2	1	$1.088 \cdot 10^{-2}$	$1.088 \cdot 10^{-2}$
9	8	7	$9.372 \cdot 10^{-5}$	0	2	1	$1.023 \cdot 10^{-2}$	$1.023 \cdot 10^{-2}$
10	8	7	$9.372 \cdot 10^{-5}$	0	0	1	$1.018 \cdot 10^{-2}$	$1.018 \cdot 10^{-2}$
11	8	7	$9.372 \cdot 10^{-5}$	0	2	1	$1.016 \cdot 10^{-2}$	$1.016 \cdot 10^{-2}$
12	9	8	$9.375 \cdot 10^{-5}$	0	0	1	$7.875 \cdot 10^{-3}$	$7.875 \cdot 10^{-3}$
Mean	11.67	11	$3.008 \cdot 10^{-4}$	2.5	1.17	0.67	$1.922 \cdot 10^{-2}$	$1.922 \cdot 10^{-2}$

(b) FS

MPF	N_{order}	$N_{order,eff}$	τ_m [s]	$N_{complex,eff}$	Relative Order	$Cancellations_{PZ}$	MAE_1	MAE_2	CONFIG
1	7	7	$1.106 \cdot 10^{-3}$	2	1	0	$1.019 \cdot 10^{-2}$	$1.019 \cdot 10^{-2}$	1110
2	20	18	$6.193 \cdot 10^{-4}$	6	0	2	$3.513 \cdot 10^{-2}$	$3.513 \cdot 10^{-2}$	1111
3	17	17	$3.634 \cdot 10^{-4}$	6	1	0	$3.333 \cdot 10^{-2}$	$3.333 \cdot 10^{-2}$	1100
4	15	15	$3.603 \cdot 10^{-4}$	6	1	0	$3.289 \cdot 10^{-2}$	$3.289 \cdot 10^{-2}$	1110
5	13	13	$2.992 \cdot 10^{-4}$	4	0	0	$3.016 \cdot 10^{-2}$	$3.016 \cdot 10^{-2}$	0100
6	15	15	$2.998 \cdot 10^{-4}$	4	1	0	$2.498 \cdot 10^{-2}$	$2.498 \cdot 10^{-2}$	1110
7	7	6	$9.371 \cdot 10^{-5}$	0	2	1	$1.019 \cdot 10^{-2}$	$1.101 \cdot 10^{-2}$	0000
8	7	6	$9.371 \cdot 10^{-5}$	0	2	1	$9.886 \cdot 10^{-3}$	$1.057 \cdot 10^{-2}$	0000
9	8	7	$9.372 \cdot 10^{-5}$	0	2	1	$5.744 \cdot 10^{-3}$	$1.003 \cdot 10^{-2}$	0000
10	8	7	$9.372 \cdot 10^{-5}$	0	0	1	$5.686 \cdot 10^{-3}$	$1.014 \cdot 10^{-2}$	0000
11	8	7	$9.372 \cdot 10^{-5}$	0	2	1	$9.978 \cdot 10^{-3}$	$9.978 \cdot 10^{-3}$	0100
12	10	9	$9.372 \cdot 10^{-5}$	4	0	1	$7.335 \cdot 10^{-3}$	$7.335 \cdot 10^{-3}$	1100
Mean	11.25	10.58	$3.008 \cdot 10^{-4}$	2.67	1	0.67	$1.796 \cdot 10^{-2}$	$1.881 \cdot 10^{-2}$	

(c) 1002 (phase-domain worst case)

MPF	N_{order}	$N_{order,eff}$	τ_m [s]	$N_{complex,eff}$	Relative Order	$Cancellations_{PZ}$	MAE_1	MAE_2
1	6	6	$1.105 \cdot 10^{-3}$	2	1	0	$1.588 \cdot 10^{-2}$	$1.786 \cdot 10^{-2}$
2	8	7	$6.199 \cdot 10^{-4}$	2	1	1	$1.495 \cdot 10^{-2}$	$4.956 \cdot 10^{-2}$
3	7	7	$3.634 \cdot 10^{-4}$	2	2	0	$1.927 \cdot 10^{-2}$	$4.887 \cdot 10^{-2}$
4	7	7	$3.605 \cdot 10^{-4}$	2	2	0	$1.858 \cdot 10^{-2}$	$4.827 \cdot 10^{-2}$
5	7	7	$2.992 \cdot 10^{-4}$	0	2	0	$1.428 \cdot 10^{-2}$	$3.971 \cdot 10^{-2}$
6	7	7	$2.999 \cdot 10^{-4}$	0	0	0	$1.226 \cdot 10^{-2}$	$3.255 \cdot 10^{-2}$
7	5	5	$9.397 \cdot 10^{-5}$	0	1	0	$1.937 \cdot 10^{-2}$	$1.937 \cdot 10^{-2}$
8	5	5	$9.397 \cdot 10^{-5}$	0	1	0	$1.961 \cdot 10^{-2}$	$1.961 \cdot 10^{-2}$
9	5	4	$9.397 \cdot 10^{-5}$	0	1	1	$1.930 \cdot 10^{-2}$	$1.930 \cdot 10^{-2}$
10	5	4	$9.397 \cdot 10^{-5}$	0	1	1	$1.931 \cdot 10^{-2}$	$1.931 \cdot 10^{-2}$
11	5	5	$9.397 \cdot 10^{-5}$	0	1	0	$1.941 \cdot 10^{-2}$	$1.941 \cdot 10^{-2}$
12	5	5	$9.397 \cdot 10^{-5}$	0	1	0	$1.941 \cdot 10^{-2}$	$1.941 \cdot 10^{-2}$
Mean	6	5.75	$3.010 \cdot 10^{-4}$	0.67	1.17	0.25	$1.764 \cdot 10^{-2}$	$2.944 \cdot 10^{-2}$

5.5.1.3 TRL01

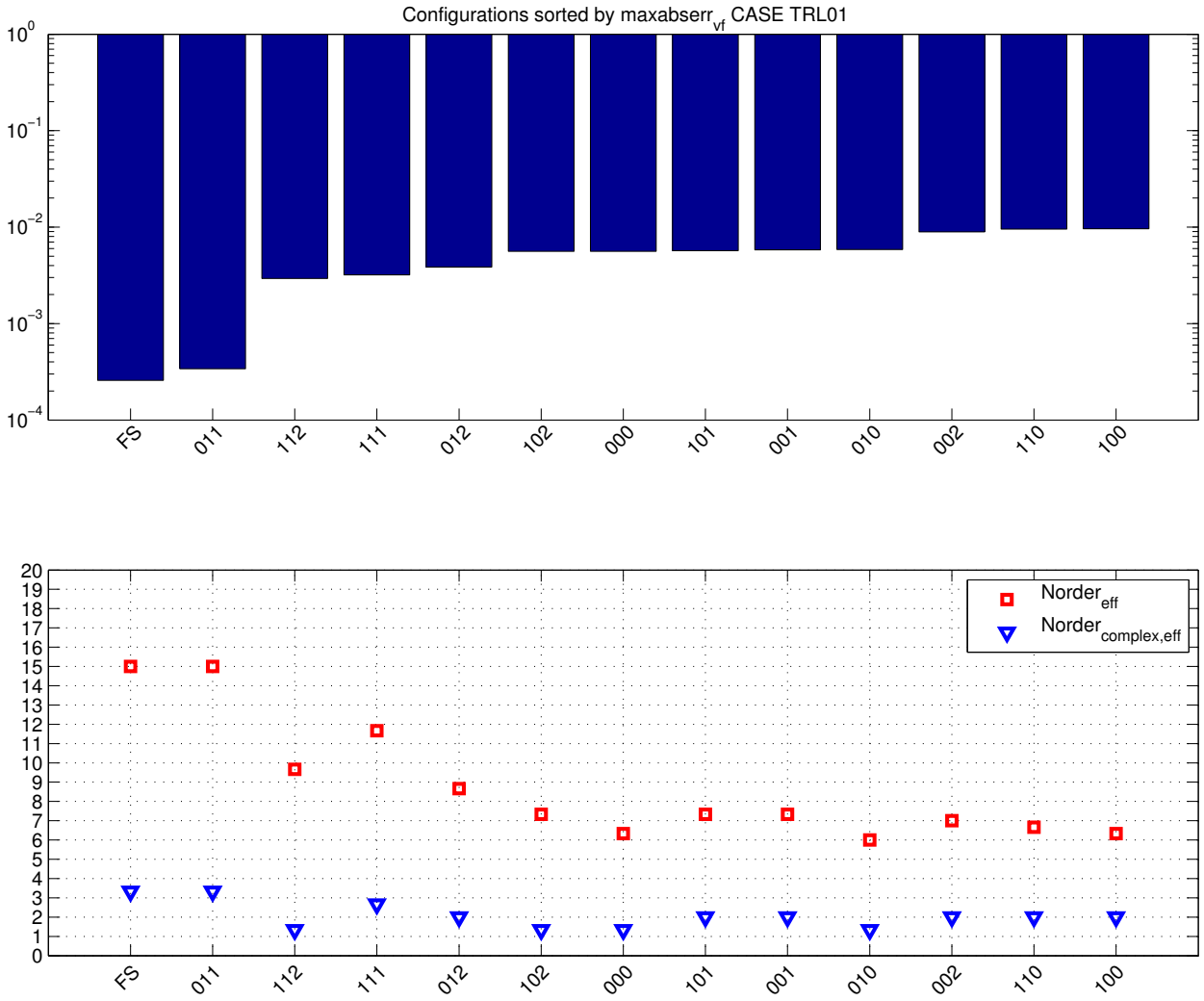

Figure 5.11: W/VF maxabserr results in the phase domain, all configurations, TRL01

Table 5.10: Select configurations, W/VF, TRL01

(a) 011 (phase-domain best case)

MPF	N_{order}	$N_{order,eff}$	τ_m [s]	$N_{complex,eff}$	Relative Order	$Cancellations_{PZ}$	MAE_1	MAE_2	RHP Zeros
1	21	20	$7.053 \cdot 10^{-3}$	6	1	1	$7.658 \cdot 10^{-4}$	$8.453 \cdot 10^{-4}$	4
2	14	14	$6.696 \cdot 10^{-3}$	4	1	0	$5.101 \cdot 10^{-4}$	$5.212 \cdot 10^{-4}$	2
3	12	11	$6.672 \cdot 10^{-3}$	0	1	1	$1.949 \cdot 10^{-4}$	$2.023 \cdot 10^{-4}$	2
Mean	15.67	15	$6.807 \cdot 10^{-3}$	3.33	1	0.67	$4.903 \cdot 10^{-4}$	$5.229 \cdot 10^{-4}$	2.67

(b) FS

MPF	N_{order}	$N_{order,eff}$	τ_m [s]	$N_{complex,eff}$	Relative Order	$Cancellations_{PZ}$	MAE_1	MAE_2	RHP Zeros	CONFIG
1	21	20	$7.357 \cdot 10^{-3}$	6	1	1	$5.155 \cdot 10^{-5}$	$5.155 \cdot 10^{-5}$	2	111
2	14	14	$6.696 \cdot 10^{-3}$	4	1	0	$5.101 \cdot 10^{-4}$	$5.212 \cdot 10^{-4}$	2	011
3	11	11	$6.672 \cdot 10^{-3}$	0	1	0	$1.609 \cdot 10^{-4}$	$1.609 \cdot 10^{-4}$	2	112
Mean	15.33	15	$6.908 \cdot 10^{-3}$	3.33	1	0.33	$2.408 \cdot 10^{-4}$	$2.445 \cdot 10^{-4}$	2	

(c) 100 (phase-domain worst case)

MPF	N_{order}	$N_{order,eff}$	τ_m [s]	$N_{complex,eff}$	Relative Order	$Cancellations_{PZ}$	MAE_1	MAE_2	RHP Zeros
1	5	5	$7.571 \cdot 10^{-3}$	2	1	0	$1.190 \cdot 10^{-2}$	$1.190 \cdot 10^{-2}$	0
2	7	7	$6.700 \cdot 10^{-3}$	2	1	0	$3.166 \cdot 10^{-3}$	$3.166 \cdot 10^{-3}$	2
3	7	7	$6.670 \cdot 10^{-3}$	2	1	0	$1.168 \cdot 10^{-2}$	$1.168 \cdot 10^{-2}$	2
Mean	6.33	6.33	$6.981 \cdot 10^{-3}$	2	1	0	$8.917 \cdot 10^{-3}$	$8.917 \cdot 10^{-3}$	1.33

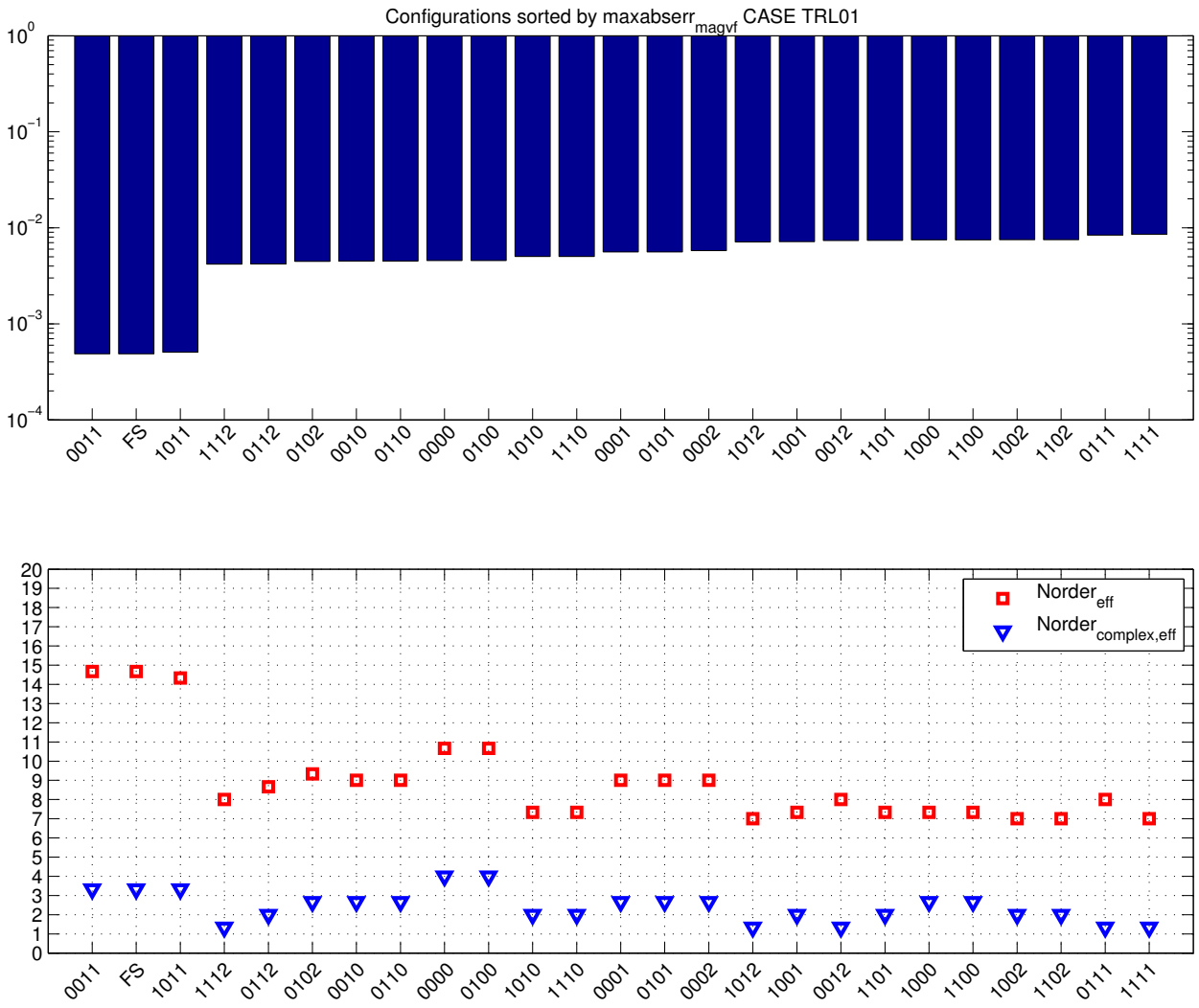

Figure 5.12: W/magVF maxabserr results in the phase domain, all configurations, TRL01

Table 5.11: Select configurations, W/magVF, TRL01

(a) 0011 (phase-domain best case)

MPF	N_{order}	$N_{order,eff}$	τ_m [s]	$N_{complex,eff}$	Relative Order	$Cancellations_{PZ}$	MAE_1	MAE_2
1	16	15	$7.488 \cdot 10^{-3}$	4	2	1	$7.794 \cdot 10^{-4}$	$1.310 \cdot 10^{-3}$
2	20	16	$6.698 \cdot 10^{-3}$	4	1	4	$1.790 \cdot 10^{-4}$	$1.427 \cdot 10^{-3}$
3	14	13	$6.673 \cdot 10^{-3}$	2	1	1	$5.492 \cdot 10^{-4}$	$1.099 \cdot 10^{-3}$
Mean	16.67	14.67	$6.953 \cdot 10^{-3}$	3.33	1.33	2	$5.025 \cdot 10^{-4}$	$1.279 \cdot 10^{-3}$

(b) FS

MPF	N_{order}	$N_{order,eff}$	τ_m [s]	$N_{complex,eff}$	Relative Order	$Cancellations_{PZ}$	MAE_1	MAE_2	CONFIG
1	16	15	$7.488 \cdot 10^{-3}$	4	2	1	$7.794 \cdot 10^{-4}$	$1.310 \cdot 10^{-3}$	0011
2	20	16	$6.698 \cdot 10^{-3}$	4	1	4	$1.790 \cdot 10^{-4}$	$1.427 \cdot 10^{-3}$	0011
3	14	13	$6.673 \cdot 10^{-3}$	2	1	1	$5.492 \cdot 10^{-4}$	$1.099 \cdot 10^{-3}$	0011
Mean	16.67	14.67	$6.953 \cdot 10^{-3}$	3.33	1.33	2	$5.025 \cdot 10^{-4}$	$1.279 \cdot 10^{-3}$	

(c) 1111 (phase-domain worst case)

MPF	N_{order}	$N_{order,eff}$	τ_m [s]	$N_{complex,eff}$	Relative Order	$Cancellations_{PZ}$	MAE_1	MAE_2
1	7	7	$7.494 \cdot 10^{-3}$	2	1	0	$4.254 \cdot 10^{-3}$	$4.254 \cdot 10^{-3}$
2	7	7	$6.699 \cdot 10^{-3}$	2	1	0	$7.959 \cdot 10^{-3}$	$7.959 \cdot 10^{-3}$
3	7	7	$6.674 \cdot 10^{-3}$	0	1	0	$1.149 \cdot 10^{-2}$	$1.149 \cdot 10^{-2}$
Mean	7	7	$6.956 \cdot 10^{-3}$	1.33	1	0	$7.902 \cdot 10^{-3}$	$7.902 \cdot 10^{-3}$

5.5.2 Discussion

From the phase-domain results, the following observations can be noted.

5.5.2.1 Comparison between W/VF and W/magVF based fitting

Some key observations from comparing the W/VF with the W/magVF results are as follows.

- W/VF, as it has been implemented here, out-performed the implementation W/magVF in terms of the individual modal as well as the final phase domain figures of merit.
- W/magVF does not bind the relative order as strictly as W/VF does. For each case, the W/VF fitter always returned a relative order of 1, while for the W/magVF fitter this value was as low as 0 and as high as 2.
- W/magVF can guarantee MPS while W/VF does not. For each case, poles could be found in the RHP for some modes, whereas for W/magVF this was not possible due to the method employed for reducing from the magnitude-squared approximation.

- W/magVF excels in its ability to extract time delays yielding comparable results with W/VF within less time and computational overhead.

5.5.2.2 Choosing different fitting parameters can be used to find the best compromise in terms of order, error, and complexity

The tests described in this section show how different settings can be used to provide approximations that satisfy a range of constraints. For instance, reducing the order, and more specifically, the number of complex poles can aid in simplifying the time-domain convolutions. Choosing the best configuration that can do this, within a desired margin of error can be quite useful.

5.5.2.3 The cable cases did not behave as expected in terms of final sweep performance, while the transmission line case did

When applying the heterogeneous final sweep, cases CAB01 and CAB02 did not behave as expected. The expected result would be that the final sweep would yield the best performance, as it mixed the MPF configurations such that the best one was chosen for each MPF, and then using the poles and delays that correspond with each to perform the phase-domain fitting. The expected behaviour was true of the TRL01 case. However, for the cable cases (using both types of fitters), the observed behaviour was that the best results were achieved through homogeneous configurations, and the final sweep performance, while close, was worse.

This observation could be rooted in the fact that cable modal decomposition is significantly more complicated than for transmission lines[18, 28, 6]. For cables, the transformation matrices used to extract the MPF's is very much frequency dependant, while for transmission lines the transformation matrices are relatively constant. It implies that the ULM decomposition methods may need to consider additional parameters, besides poles and delays in the modal domain, when composing the propagation function matrices. Improvements to the ULM, or perhaps to the specific implementation used, may be warranted in this regard.

5.5.2.4 Robust fitting

Even though various fitting parameters were modified, the overall fitness between best and worst cases was within two orders of magnitude. This illustrates that these fitters are quite robust. They can withstand different types of numerical perturbations, and yet still return accurate approximations.

CHAPTER 6

CONCLUSIONS

6.1 Review of methodology

This thesis has taken an in-depth analysis of the magVF algorithm, specifically with the intentions of applying this technique toward modelling of cables and transmission lines using the ULM.

The study begins with a review of the academic record, to study the state of the art of fitting in the context of transmission line and cable propagation function modelling. Details about the procedure has been provided, with theoretical background and practical implementations. Included in these is the development of an iteratively updating weighting method called WmagVF, which is based on the synthesis of WVF theory with magVF, and a pole modification scheme designed to bias the iterative solution toward specific types of responses. Specific details, such as a procedure for performing pole-zero cancellations to reduce overall complexity, use of Disciplined Convex Programming for optimizing residues to create realizable approximations, and algorithms for different approaches to fitting are also provided.

Results are given using arbitrary transfer functions which are known and selected specifically to study the strengths and weaknesses of the implemented algorithms. Next, a series of intensive investigations into the application of W/magVF is performed in the modal domain with a single cable case. Finally, an extensive study is performed using an automated procedure and up to 27 different configurations is run, with up to 20 poles per modal propagation function, to determine how the modal domain fitness relates to the fitness of approximation in the phase domain, based on the the theory of the Universal Line Model.

6.2 Summary of findings

The following list provides some of the important findings of this study.

- Weighting, Input Pole Modification, and restriction of the convergence to magnitudes can be useful for helping certain MPFs to converge on a solution, and have different effects depending on the case in which they are used. Experimenting with different configurations can be useful for trying to find the best compromise between order, accuracy, and complexity.

- Delay determination in magVF is quick and accurate

- The VF, and magVF based methods, suffer from an inability to accurately approximate repeated poles.
- Pole-zero cancellation can be used to help reduce the burden of the overall approximation order.
- W/magVF does not restrict the relative order of the approximation, while VF does.
- W/magVF can inherently guarantee MPS approximations while W/VF does not.
- Both fitters are robust and highly effective, and can withstand inter-iteration perturbations while maintaining their abilities to converge on accurate solutions.
- Fitting cables using the ULM is more complicated than fitting transmission lines, as better modal-domain fitness did not imply better phase-domain results for the cable cases. On the contrary, the transmission line case did behave as expected in this regard.

6.3 Proposed avenues of enquiry for future research

6.3.1 More selective application of Input Pole Modification

It could be interesting to develop a more refined approach to the application of IPM. For instance, if at certain frequencies there is a resonant peak, or large phase shift, then perhaps trying to place real poles in the relevant frequency range would be counter-productive. Similarly, the IPM technique could be modified to help fit situations where repeated poles may exist on the real axis, by injecting small imaginary parts to a pair of complex poles. In this way, the limitations observed with trying to fit repeated poles using first-order pole-residues basis functions may be circumvented. Also studies should be made to see if using such a technique to inject imaginary components to the incoming poles can help to fit systems with resonant peaks.

6.3.2 Further analysis of alternatives to ULM transformation matrices for cables

As has been demonstrated in Section 5.5, the fitting of cables using ULM procedure can be improved. It would appear that modal domain poles and time delays are not the only components that are required to properly approximate the phase domain propagation matrix. The frequency dependence of the transformation matrices used to convert from the phase to the modal domain could be a source of the additional error observed, as compared to the transmission line cases. Further research should be conducted to investigate this phenomenon, and understand how to improve the approximation procedure accordingly.

6.3.3 Swapping of zeros and poles across imaginary axis for fitting non-minimum phase transfer functions from magnitude-squared approximation

It would be interesting to develop an efficient algorithm for swapping zeros (or in the case of unstable systems, poles as well) across the imaginary axis to see how a transfer function which is non-minimum phase could be approximated using the W/magVF method. Efficiency can be gained by trying to first analyze the difference between the approximated response and the desired response, and then see where these differences are most apparent. Then, by estimating the frequency range in which mixed-phase poles and zeros may lie – by using principles of asymptotic bode plotting – swapping poles and zeros from the LHP to the RHP can commence, with checks being made for improvements, or worsening, of the approximation.

6.3.4 Exploitation of LTI MPS/All-Pass decomposition for correcting phase of approximation

Theoretically, all LTI systems can be decomposed into a minimum-phase component which fully characterizes the magnitude response, and an all-pass component which has a unity magnitude [29] but may have some frequency dependent phase response. Note that, the entire phase response will need to include the MPS component's response as well as the phase response of the all-pass component.

For a mixed-phase system, the all-pass filter will contain the RHP zeros, for a minimum-phase system the all-pass filter will not exist. For a delayed minimum-phase system, the exponential with the delay is the all-pass component, as it modifies the phase and has a unity magnitude. It would be interesting to see if such decomposition methods could be used to help correct the phase of a mixed-phase system using a MPS approximation as a starting point and augmenting it with an appropriate all-pass filters, the most simple of these being the pure delay, independent of frequency. Frequency dependent all-pass filters may need to also be considered in more complicated cases.

6.3.5 Combining W/magVF with W/VF in an overall fitting procedure

W/VF suffers from poor fitting when the delay is not accounted for. On the other hand, W/magVF is able to fit the magnitude-squared response and then, by reducing the regular response (ie., not magnitude-squared), is able to very simply find a good approximation for the delay. However, the W/magVF method does not yet give as good results for the poles and residues as W/VF does. It would be interesting to see if W/magVF can be used to find the MPF time delays, and then these results can be used with W/VF to find a good

approximation of the poles, and if necessary, residues of the approximated system. This method could speed up the overall system approximation process since the delays would not need to be determined in a root-finding algorithm. The overall timing of the solution could be controlled and this could be useful, for example, in real-time calculation systems which need to have strict limits defined for the compute durations.

6.4 Concluding remarks

This thesis elaborates on the theory required for – and provides successful demonstrations of – an implementation of the magVF method for the identification of power system transfer functions. Additionally, this study provides the derivation of WmagVF, a new variation that employs iterative weighting, analogous to the WVF method. Selective modifications are also exploited as required to improve the convergence of the fit of the magnitudes for troublesome functions. It is observed that: W/magVF can converge quicker than W/VF in certain cases; W/magVF can implicitly guarantee minimum-phase approximations while W/VF cannot; delay determination is trivial in W/magVF compared to W/VF; and pole modification schemes and weighting can have a beneficial impact on the convergence and order of the fit. These results can be used to further improve the modelling and analysis of transmission line and cables.

BIBLIOGRAPHY

[1] B. Gustavsen and A. Semlyen, "Rational approximation of frequency domain responses by vector fitting," *Power Delivery, IEEE Transactions on*, vol. 14, pp. 1052–1061, Jul 1999.

[2] C. Sanathanan and J. Koerner, "Transfer function synthesis as a ratio of two complex polynomials," *Automatic Control, IEEE Transactions on*, vol. 8, pp. 56 – 58, Jan 1963.

[3] E. Levy, "Complex curve fitting," *Automatic Control, IRE Transactions on*, vol. 4, pp. 37 – 44, May 1959.

[4] A. Semlyen and B. Gustavsen, "Vector fitting by pole relocation for the state equation approximation of nonrational transfer matrices," *Circuits Systems And Signal Processing*, vol. 19, no. 6, pp. 549–566, 2000.

[5] B. Gustavsen and A. Semlyen, "Enforcing passivity for admittance matrices approximated by rational functions," *Power Systems, IEEE Transactions on*, vol. 16, pp. 97 –104, Feb 2001.

[6] B. Gustavsen, "Computer code for rational approximation of frequency dependent admittance matrices," *Power Delivery, IEEE Transactions on*, vol. 17, pp. 1093 – 1098, Oct 2002.

[7] B. Gustavsen and A. Semlyen, "A robust approach for system identification in the frequency domain," *Power Delivery, IEEE Transactions on*, vol. 19, pp. 1167 – 1173, July 2004.

[8] B. Gustavsen, "Improving the pole relocating properties of vector fitting," *Power Delivery, IEEE Transactions on*, vol. 21, pp. 1587 –1592, July 2006.

[9] I. Kocar, J. Mahseredjian, and G. Olivier, "Weighting method for transient analysis of underground cables," *Power Delivery, IEEE Transactions on*, vol. 23, pp. 1629 –1635, July 2008.

[10] I. Kocar, J. Mahseredjian, and G. Olivier, "Improvement of numerical stability for the computation of transients in lines and cables," *Power Delivery, IEEE Transactions on*, vol. 25, pp. 1104 –1111, April 2010.

[11] L. De Tommasi, B. Gustavsen, and T. Dhaene, "Robust transfer function identification via an enhanced magnitude vector fitting algorithm," *Control Theory Applications, IET*, vol. 4, pp. 1169 –1178, July 2010.

[12] L. de Tommasi and B. Gustavsen, "Low order transmission line modeling by modal decomposition and minimum phase shift fitting," in *Signal Propagation on Interconnects, 2006. IEEE Workshop on*, pp. 89 –92, May 2006.

[13] L. De Tommasi, *Identification of Broadband Passive Macromodels of Electromagnetic Distributed Structures*. PhD thesis, Università di Napoli Federico II, 2006.

[14] L. de Tommasi, B. Gustavsen, and T. Dhaene, "Accurate macromodeling based on tabulated magnitude frequency responses," in *Signal Propagation on Interconnects, 2008. SPI 2008. 12th IEEE Workshop on*, pp. 1 –4, May 2008.

[15] W. Hendrickx, D. Deschrijver, L. Knockaert, and T. Dhaene, "Magnitude vector fitting to interval data," *Math. Comput. Simul.*, vol. 80, pp. 572–580, November 2009.

[16] M. Jong and K. Shanmugam, "Determination of a transfer function from amplitude frequency response data," *International Journal of Control*, vol. 25, no. 6, pp. 941 – 948, 1977.

[17] Z. Zhang, G. Liang, X. Cui, and M. Wu, "A high frequency transfer function model of potential transformer in GIS," in *Electromagnetic Compatibility, 2002 3rd International Symposium on*, pp. 186 – 189, May 2002.

[18] J. Marti, "Accurate modelling of frequency-dependent transmission lines in electromagnetic transient simulations," *Power Apparatus and Systems, IEEE Transactions on*, vol. PAS-101, pp. 147 –157, jan. 1982.

[19] A. Morched, B. Gustavsen, and M. Tartibi, "A universal model for accurate calculation of electromagnetic transients on overhead lines and underground cables," *Power Delivery, IEEE Transactions on*, vol. 14, pp. 1032 –1038, Jul 1999.

[20] B. Gustavsen and J. Nordstrom, "Pole identification for the universal line model based on trace fitting," *Power Delivery, IEEE Transactions on*, vol. 23, pp. 472 –479, Jan 2008.

[21] M. Grant and S. Boyd, "Graph implementations for nonsmooth convex programs," in *Recent Advances in Learning and Control* (V. Blondel, S. Boyd, and H. Kimura, eds.), Lecture Notes in Control and Information Sciences, pp. 95–110, Springer-Verlag Limited, 2008.

[22] CVX Research, Inc., "CVX: Matlab software for disciplined convex programming, version 2.0 beta." `http://cvxr.com/cvx`, Sept. 2012.

[23] I. Kocar, *Wideband modeling of transmission lines and cables.* PhD thesis, École Polytechnique de Montréal, 2009.

[24] D. Deschrijver and T. Dhaene, "A note on the multiplicity of poles in the vector fitting macromodeling method," *Microwave Theory and Techniques, IEEE Transactions on*, vol. 55, no. 4, pp. 736–741, 2007.

[25] O. Ramos-Leanos, J. Naredo, J. Mahseredjian, C. Dufour, J. Gutierrez-Robles, and I. Kocar, "A wideband line/cable model for real-time simulations of power system transients," *Power Delivery, IEEE Transactions on*, vol. 27, no. 4, pp. 2211–2218, 2012.

[26] H. Bode, *Network Analysis and Feedback Amplifier Design.* Bell Telephone Laboratories series, Van Nostrand, 1945.

[27] T. Quatieri Jr and A. Oppenheim, "Iterative techniques for minimum phase signal reconstruction from phase or magnitude," *Acoustics, Speech and Signal Processing, IEEE Transactions on*, vol. 29, no. 6, pp. 1187–1193, 1981.

[28] T. Noda, N. Nagaoka, and A. Ametani, "Phase domain modeling of frequency-dependent transmission lines by means of an ARMA model," *Power Delivery, IEEE Transactions on*, vol. 11, pp. 401 –411, Jan 1996.

[29] A. V. Oppenheim, R. W. Schafer, and J. R. Buck, *Discrete-time signal processing (2nd ed.).* Upper Saddle River, NJ, USA: Prentice-Hall, Inc., 1999.